Journal of Sedimentary Research

Journal of Sedimentary Research, 2014, v. 84, 988–1004
Research Article
DOI: http://dx.doi.org/10.2110/jsr.2014.80

FRESHWATER LIMESTONE IN AN ARID RIFT BASIN: A GOLDILOCKS EFFECT

GAIL M. ASHLEY,[1] CAROL B. DE WET,[2] MANUEL DOMÍNGUEZ-RODRIGO,[3] ALYSSA M. KARIS,[1] THERESA M. O'REILLY,[2] AND RONIDELL BALUYOT[1]

[1]*Earth and Planetary Sciences, Rutgers University, 610 Taylor Road, Piscataway, New Jersey 08854-8066, U.S.A.*
[2]*Earth & Environment, Franklin & Marshall College, 415 Harrisburg Avenue, Lancaster, Pennsylvania 17604-3003, U.S.A.*
[3]*Department of Prehistory, Complutense University, Prof. Aranguren s/n, 28040 Madrid, Spain*
e-mail: gmashley@rci.rutgers.edu

ABSTRACT: **The Olduvai Basin (3° S), situated just west of the East African Rift System in northern Tanzania, contains a two-million-year record of paleoclimate and paleoenvironmental change, as well as a rich archive of vertebrate paleontology (including hominins). Milankovitch precession cycles (~ 20 kyr) regulate the mean annual precipitation (250–700 mm/yr), and the ~ 2500 mm/yr evapotranspiration results in a negative hydrologic balance. Despite persistent aridity, extensive deposits of freshwater limestone punctuate the stratigraphic record. Between 2 and 1 Ma, Lake Olduvai occupied the basin, and its sediments are a proxy for climate-driven cycles. Three limestones (1.84, 1.80, and 1.36 Ma in age), which formed within lake-margin floodplains adjacent to the lake, were studied to determine their depositional environment using field relations, sedimentary structures, fossils, petrography, and stable-isotope and major-element geochemistry. The three limestones are similar in that they contain peloidal micrite, siliciclastic detrital grains, and rhizoconcretions. Abundant faunal remains (gastropods, ostracods, *Charaphytes*, and fish) indicate that ponded water was relatively fresh and alkaline.**

Geochemical and stable-isotope data indicate two types of groundwater-sourced carbonate-producing waters: a deeper-sourced fluid that was enriched in iron and manganese due to extended water–rock interactions, and a shallower groundwater that traveled through alluvial-fan deposits. Regional faults tapped the deeper groundwater, producing carbonate at spring sites, while seeps associated with basinward changes in alluvial-fan slopes drew on shallower groundwater sources. Isotope compositions indicate that fault-related waters experienced some evaporation as water moved away from the spring sites while compositions of the seep-related carbonate remained relatively constant. Pedogenic alteration and meteoric calcite cementation affected the carbonate when the spring and seep sites dried out. Secondary strontium-rich dolomite precipitated within the limestones during burial under paleo–Lake Olduvai sediments and fluids during periods of lake expansion.

Integrating these data within the geological context of regional paleoclimatic and local environmental change indicates that the freshwater carbonates formed periodically when the conditions were just right, i.e., a "Goldilocks Effect." Carbonates near the basin center formed from groundwater flowing under a hydraulic head from faults or fractures during the falling limbs of Milankovitch cycles when the lake was in recession. Carbonates near the basin margin formed from an increased rate of groundwater seepage that occurred only on the rising limbs of cycles. In both contexts, the continuous flow of groundwater with surface evaporation and CO_2 degassing optimizes the conditions for limestone formation in this arid environment. These results help explain the formation of freshwater limestones in the rift basin, link the carbonates to specific portions of Milankovitch cycles, and document that localized sources of potable water were present for use by hominins in Olduvai Gorge during an important period of human evolution.

INTRODUCTION

The Olduvai Basin is situated in northern Tanzania on the margin of the East African Rift System (EARS) (Fig. 1). Olduvai Gorge is world famous because of the hominin fossils discovered in the 1950s by Louis and Mary Leakey (Leakey 1959). The Gorge contains detailed paleontological and archaeological records which are a unique resource for studies of human origins (Leakey 1971; Blumenschine et al. 2003; Domínguez-Rodrigo et al. 2007). The Pleistocene-age deposits are a 100-meter-thick sequence of volcaniclastics, tuffs, and thin carbonates (Fig. 2A) that archive a rich record of plants, vertebrate fossils (including four hominin species), and thousands of stone tools that were used for accessing food (Leakey 1971; Bunn and Kroll 1986).

The purpose of this research is to (1) determine the depositional environment(s) of limestone formation in an arid–hyperarid setting, (2) determine the relationship between limestone formation and Milankovitch climate cycles, and (3) document the occurrence of fresh-water sources available to early hominins. Understanding how the limestones formed, where they formed in the basin, and when they formed with respect to climate are important to both geological and anthropological communities in that they provide new insights into climate-driven cyclic deposition, and how our ancestors may have been able to take advantage of environments produced during changing climatic conditions.

Richard L. Hay developed a geological model for the basin that included a playa lake in a closed depression (Hay 1976; Hay and Kyser

Published Online: November 2014
 1527-1404/14/084-988/$03.00

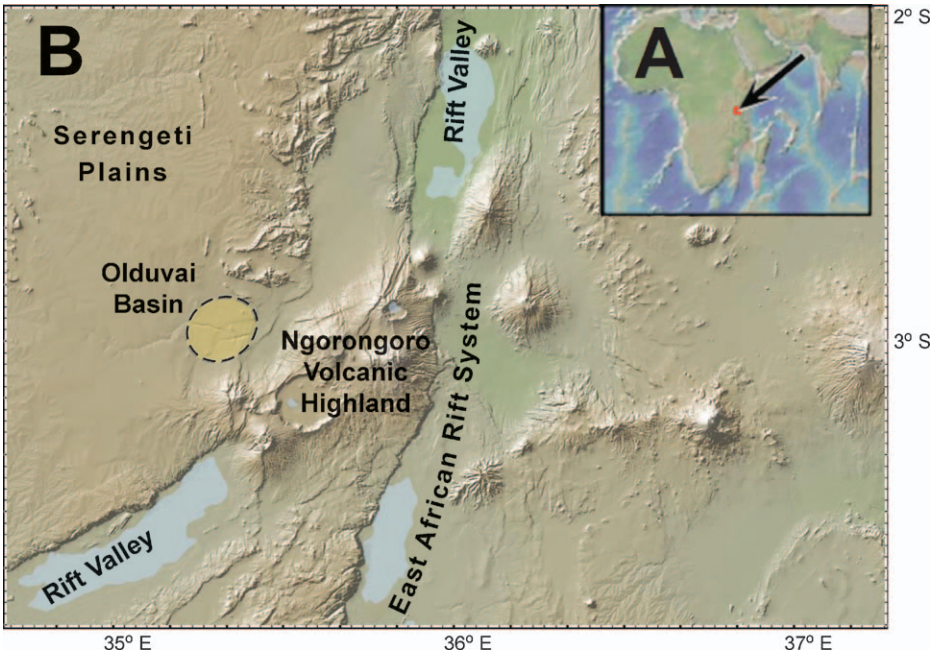

FIG. 1.—Regional location map. **A)** Inset map of Africa, arrow indicates location of study. **B)** DEM image of the East African Rift System in northern Tanzania. Olduvai Basin was situated between the Ngorongoro Volcanic Highland and the Serengeti Plain. Olduvai Gorge, an incision into the basin sediments, shows faint traces of the eastward draining modern Olduvai River. GeoMapApps.

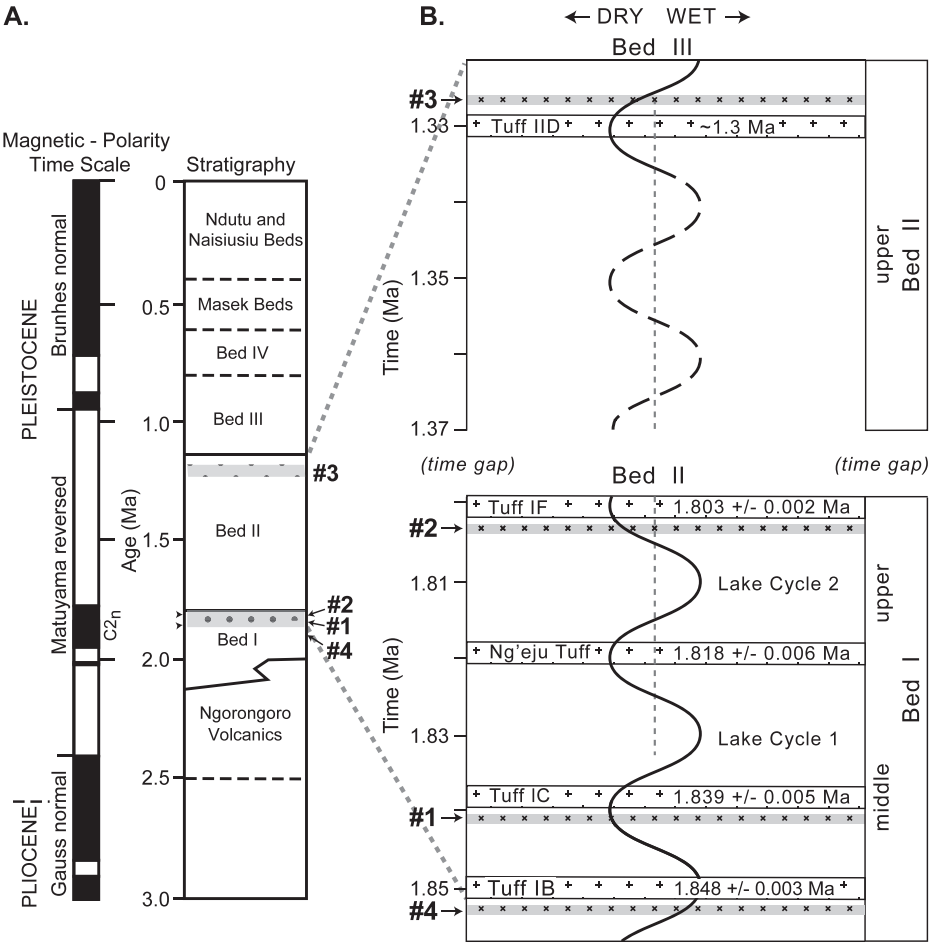

FIG. 2.—**A)** Geologic column. Magnetic-polarity time scale and stratigraphy of Olduvai Gorge. The relative stratigraphic positions of three limestones (#1, #2, and #3) that were analyzed in this study are indicated (modified from Hay 1976). **B)** Climate cycles. Diagrammatic depiction of the timing of the precession driven wet–dry climate cycles that impacted lake levels in the basin. The position of Limestone #4 is shown at the bottom of the sequence. The timing of wet–dry periods of Bed I is based on lithologically determined lake cycles (Ashley 2007) and from stable hydrogen-isotope composition from lipid biomarkers (Magill et al. 2012b) constrained by dated tuffs (Deino 2012). The timing of wet–dry periods of Bed II is more speculative, but is based on lithologically determined lake cycles indicated by solid line (Ashley 2012) and related to a dated tuff (Hay 1976). Dashed line shows timing of climate cycle based on assumption of the continuation of a long-term pattern.

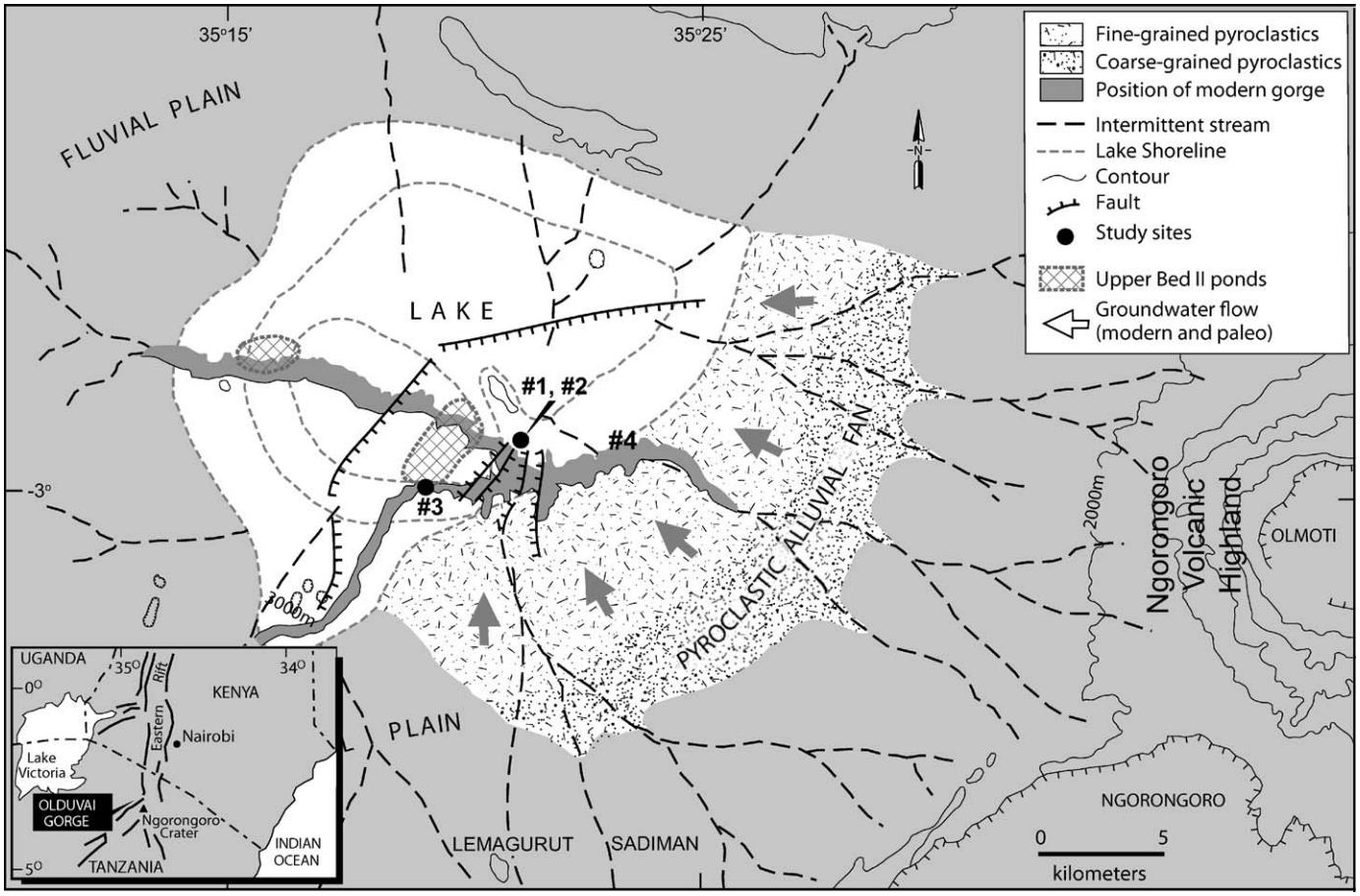

FIG. 3.—Section location map. Inset shows the location of the Olduvai Gorge in East Africa. The map is a paleogeographic reconstruction of the Olduvai Basin during Bed I and Bed II time showing interpreted flow paths (arrows) of groundwater from the Ngorongoro Volcanic Highland. Also shown are the outline of various lake levels (dashed lines), the restricted location of the Upper Bed II ponds (hachured), interpreted position of intermittent streams, key faults, and the limestone localities (#1, #2, #3, and #4). Modified from Ashley and Hay (2002).

2001). During the Pleistocene, the Olduvai Basin gradually filled with lava flows, air-fall tuffs, and reworked volcaniclastic sediment from the Ngorongoro Volcanic Highland to the east and fluvial sediments from the Serengeti Plain that lie to the west (Fig. 1). Stratigraphic nomenclature was established by Mary Leakey (Leakey 1971), and thus each unit termed "Bed" actually represents a relatively thick (meters to tens of meters thick) stratigraphic section containing multiple beds in the geological sense, spanning thousands of years (Fig. 2A). Subsequent research has determined that the lake expanded and contracted in response to astronomically driven (precession) climate cycles (Ashley 2007; Magill et al. 2012a) (Figs. 2B, 3). Olduvai Basin is similar to other rift basins situated near the equator that archive evidence of astronomically driven climate cycles (Olsen 1986; Deino et al. 2006). Interpreted paleo-precipitation ranges annually from 250 to 700 mm/yr over an ~ 20,000 year precession cycle, and combined with the estimated evapotranspiration (~ 2,000–2,500 mm/yr) indicate a persistently negative hydrologic budget (Magill et al. 2012b). These conditions exist now, as well as during the last two million years. Rift-related tectonics caused the Olduvai River to incise through the basin sediment package, creating the Olduvai Gorge (Fig. 3).

The Olduvai stratigraphy is important to our understanding of human biological and behavioral evolution. Paleoenvironmental studies have helped unravel the changes of the landscape using the clastic record in between the tuffs (Ashley and Hay 2002; Ashley 2007b; Barboni et al. 2010). However, the abundant occurrences of carbonates have received little attention except for specialized studies of calcretes (Hay and Reeder 1978), carbonate paleosols (Cerling and Hay 1986; Sikes and Ashley 2007), and diagenetic nodules and cements (Bennett et al. 2012). Carbonates associated with hominin-bearing archaeological sites (Ashley et al. 2009; Ashley et al. 2010b; Ashley et al. 2010a) are particularly important because they appear to record fresh-water sources in this arid to hyperarid setting.

Early workers in the Gorge assumed that the concentration of archaeological material was linked to paleo–Lake Olduvai (Leakey 1971; Hay 1976). However, geochemical and mineralogical studies of the lake sediments reveal that the lake was a saline–alkaline playa and an implausible source of freshwater for animals, including hominins (Hay and Kyser 2001; Hover and Ashley 2003; Deocampo et al. 2009). Investigations initiated in 2007 by TOPPP (The Olduvai Paleoanthropology and Paleoecology Project) yielded a number of carbonate deposits between ~ 1.9 and 1.3 Ma. These deposits, referred to as Middle Bed I, Upper Bed I, and Upper Bed II, had not been studied in detail by previous researchers, even though all have archaeological remains in close physical proximity (Ashley et al. 2010c).

These carbonate strata occur in three distinct stratigraphic horizons, and their ages are well constrained by ^{40}Ar–^{39}Ar dates from associated tuff beds (Fig. 2B) (Deino 2012) Preliminary field work has identified a fourth horizon of carbonate (#4 under Tuff IB within Middle Bed I) (Fig. 2B). With respect to their occurrence in time and space, all of them are limited in terms of where they occur within the basin and when they

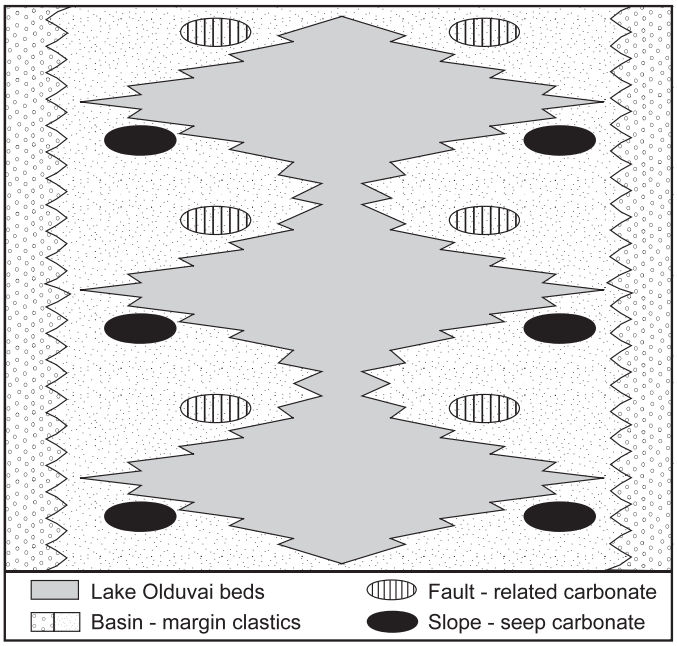

FIG. 4.—Schematic time and space diagram of lithofacies. Clastics fringe the 40-km-wide basin. Lake Olduvai beds expanded and contracted as a function of 19 to 23 kyr precession-driven cycles. Fault-related carbonates are found near the basin center and only during the falling limb of the cycle, whereas seep-related carbonates occur closer to the margin of the basin and only during the rising limb of the cycle.

were deposited within the Milankovitch cycle (Fig. 4). This paper presents new geologic data (field relations, sedimentary structures, fossils, carbonate petrography) and geochemical data (elemental abundance and stable isotopes) obtained from three carbonate deposits and determines their paleoenvironmental and paleoclimatic context. Synthesis of all data elucidates fluid pathways and clarifies the role of nonlacustrine water as sources of potable water for hominins and animals.

BACKGROUND

Basin Geology and Geomorphology

Olduvai Gorge is an incised river system draining eastward toward the Ngorongoro Volcanic Highland, a large volcanic complex composed of a number of volcanoes that have been active for over five million years (Dawson 2008; Mollel et al. 2011; Deino 2012). The Gorge dissects a sedimentary basin that is situated on the rift margin; the basin is not in the rift system (Fig. 1). When formed, the Olduvai Basin was roughly circular, ~ 50 km wide, and shallow (100 m). A lake occupied the basin center from 2 to1 Ma and shrank as infilling progressed (1 to 0 Ma). The basin's well-dated tuffs allow basin-wide correlation of widely separated outcrops and dating of archaeological sites (Blumenschine et al. 2003; McHenry 2005; Deino 2012). Rift-related extensional tectonics segmented the Olduvai stratigraphy into blocks separated mainly by normal faults (Hay 1976). Extensional tectonics and volcanism is part of a regional response to the ongoing development of the EARS (Foster et al. 1997; Dawson 2008; Le Gall et al. 2008). As documented in other rift-basin localities such as the Mesozoic eastern North American rift-basins (Birney de Wet and Hubert 1989; de Wet et al. 2002) and the Plio-Pleistocene southern Rio Grande Rift, USA (Mack 2000), bedrock, faults, and magmatic sources influenced groundwater composition and flow patterns at Olduvai (Ashley and Hay 2002; McHenry 2009).

Climate and Hydrology

Precipitation in the EARS varies seasonally with location, topography, and, on the long term, astronomically controlled climate cycles (Trauth et al. 2007) (Fig. 4). Estimates of precipitation in the Gorge vary from 250 mm/yr during drier portions of the precession cycle up to 700 mm/yr during wetter portions (Magill et al. 2012b). The mean annual temperature (MAT) averages 25°C and, because the site is near the equator, it likely has not varied significantly in the past. The potential evapotranspiration (PET) is four times the precipitation (~ 2000–2500 mm/yr), resulting in an annual negative hydrologic budget (Dagg et al. 1970). Few, if any, perennial rivers can persist with this negative water budget, and most rivers draining into the basin are, and were, likely intermittent and ephemeral (Hay 1976; Ashley and Hay 2002) (Fig. 3). The modern Ngorongoro Volcanic Highland, over 3000 m high, traps moisture-laden easterly winds blowing from the Arabian Sea and creates a westerly rain shadow. Modern rainfall on Ngorongoro is 1150 mm/yr (Deocampo 2004) and was perhaps twice that during precession wet periods. Some rainfall runs off in ephemeral surface streams, but most infiltrates into the porous volcaniclastic deposits of the Highland and moves westward through the subsurface into the Olduvai Basin (Fig. 3). Today, groundwater exits at the base of the slope, creating a shallow, seasonally variable (lake or wetland) water body called Obalbal. The scenario was likely similar during the Pleistocene, at which time the Ngorongoro Highland was even higher. This is, apparently, a common scenario along the EARS, as noted by Olago et al. (2009) in the Central Kenya Rift, groundwater in the basins is derived from rainfall on the valley's upland flanks. A number of previous studies of paleoclimate and paleoenvironmental reconstructions at Olduvai have recognized former springs and wetlands associated with archaeological sites in Middle Bed I (Ashley et al. 2010b), Upper Bed I (Ashley et al. 2010a; Ashley et al. 2014), and Lowermost Bed I (Liutkus and Ashley 2003; Ashley et al. 2009; Deocampo and Tactikos 2010); but here we present a unifying conceptual model to explain the reoccurrence of fresh-water carbonates in this volcaniclastics-dominated arid basin.

METHODS

Field

The stratigraphy of each of the three sites was described, logged using scaled drawings, and photographed. Representative samples were collected for analyses and the three site locations documented using global-positioning satellite (GPS) methods. Middle and Upper Bed I carbonate horizons occur stratigraphically near the top of Bed I and are closely associated with mapped faults near the middle of the present gorge (Figs. 2, 3). The carbonate horizon designated #3 (Upper Bed II) occurs stratigraphically near the top of Bed II and geographically is located southwest of carbonates #1 and #2 (Middle Bed I and Upper Bed I) (Figs. 2, 3).

Laboratory

Microscopy.—Hand samples and fifty-eight thin sections (stained with potassium ferricyanide and alizarin red-S (Dickson 1966)) were described. Scanning electron microscopy (SEM) was conducted at Franklin and Marshall College for detailed study of depositional and diagenetic textures.

X-Ray Diffraction (XRD).—Microsamples of carbonate (micrite ± sparry calcite, aragonite, and/or dolomite) were obtained using a Dremel microdrill at low rpms. Each sample was microdrilled under a magnifying glass to avoid visible clay concentrations or other obvious impurities. Samples were run at Franklin & Marshall College on a PANalytical X'pet Pro PW3040 X-ray diffraction spectrometer using Cu K Alpha radiation, an automated diffraction slit, and an X'Celerator detector, according to

FIG. 5.—Photos of outcrops. **A)** Middle Bed I. White carbonate with undulating surface is ~ 0.5 m thick and draped with an airfall tuff (Tuff IC). **B)** Upper Bed I. White carbonate (1.4 m thick) is draped with an airfall tuff (Tuff IF). Some feather-thin laminae of clay are intercalated. **C)** Upper Bed II. White carbonate (1 m thick) is overlain by a smectite-rich clay. The limestone overlies a 1-m-thick siliceous clay bed.

standard procedures (scans from 6 to 70° 2 θ and a NIST traceable Si metal used to check goniometer accuracy).

Geochemical Analysis.—The sampling technique for geochemistry is the same as for the XRD technique, i.e., microdrilled micrite, avoiding visible impurities, to obtain 0.05 g of carbonate (micrite ± sparry calcite, aragonite, and/or dolomite). Each sample was associated with thin-section analysis so that unavoidable incorporation of shells, spar, or other soluble material could be referenced to the petrography. Double samples (a, b) were taken where dolomite might be particularly likely to be incorporated. Samples were dissolved in 10% nitric acid and analyzed at Franklin & Marshall College on a SPECTROBLUE inductively coupled plasma optical emission spectrometer (ICP-OES), with 750 mm focal length, a Paschen-Runge optical system and 15 linear CCD array detectors. Calibrations were made to seven standards, diluted to appropriate concentrations, from Specpure commercial stock solutions. Results are reported in ppm.

Stable-Isotope Analysis.—Carbonate samples weighing 550 µg to 900 µg were ground to fine powder. The $\delta^{13}C$ and $\delta^{18}O$ values of carbonate samples were analyzed at Rutgers University in the Stable Isotope Laboratory in the Department of Earth and Planetary Sciences. Samples were loaded into a Multiprep device attached to a Micromass Optima mass spectrometer. The $CaCO_3$ was reacted in 100% phosphoric acid at 90°C for 800 seconds. Values are reported in standard per mil (‰) notation relative to the Vienna Pee Dee Belemnite standard (V-PDB) through the analysis of an internal laboratory standard that is routinely measured with NBS-19 calcite. We use the Coplen et al. reported values of 1.95 and −2.20‰ for $\delta^{13}C$ and $\delta^{18}O$, respectively (Coplen et al. 1983). The long-term standard deviations on the internal lab standard are 0.05 and 0.08‰ for $\delta^{13}C$ and $\delta^{18}O$, respectively.

RESULTS

Middle Bed I

Depositional Characteristics.—The undulating surface of the limestone can be traced for at least 35 m in length, forming a broad mound. It is 10 m wide and a maximum of ~ 0.5 m thick (Fig. 5A). Distal areas have a patchy distribution of carbonate intercalated with clay. The limestone overlies a clay deposit, and a thin 1-cm-thick clay layer drapes over it, which is in turn blanketed with a 30-cm-thick fine-grained air-fall tuff (Tuff lC) (Fig. 2). The limestone has a nodular, irregular fabric, and consists of chalky-textured micrite with pockets of clay and root molds. Abundant catfish, *Clarius*, bones are found in the sediments (Stewart 1994, 1996).

Petrographic Characteristics.—The limestone consists of *Charophyte* oogonia (Fig. 6A), gastropods (Fig. 6B), and ostracod shell fragments in peloidal, clotted, nonferroan micrite. Angular to subangular volcaniclastic lithic and quartz sand and silt-size grains occur in the micrite. Features that are possible plant stem or root fragments are locally preserved, and rhizoconcretions are abundant.

Diagenetic Characteristics.—The micrite matrix of Middle Bed I exhibits shrinkage fractures and circumgranular cracks. Micrite is locally aggraded to microspar with sparry calcite precipitation around root traces and in cavities. Pyrolusite is associated with rhizoconcretions, and the precipitation of blocky dolomite fills some of the final porosity, although many root molds remain uncemented. Based on crosscutting relations, dolomite is the last precipitated carbonate mineral in the paragenetic sequence. Results of X-ray diffraction indicate that most of the carbonate is calcite, with minor amounts of dolomite and aragonite (Table 1).

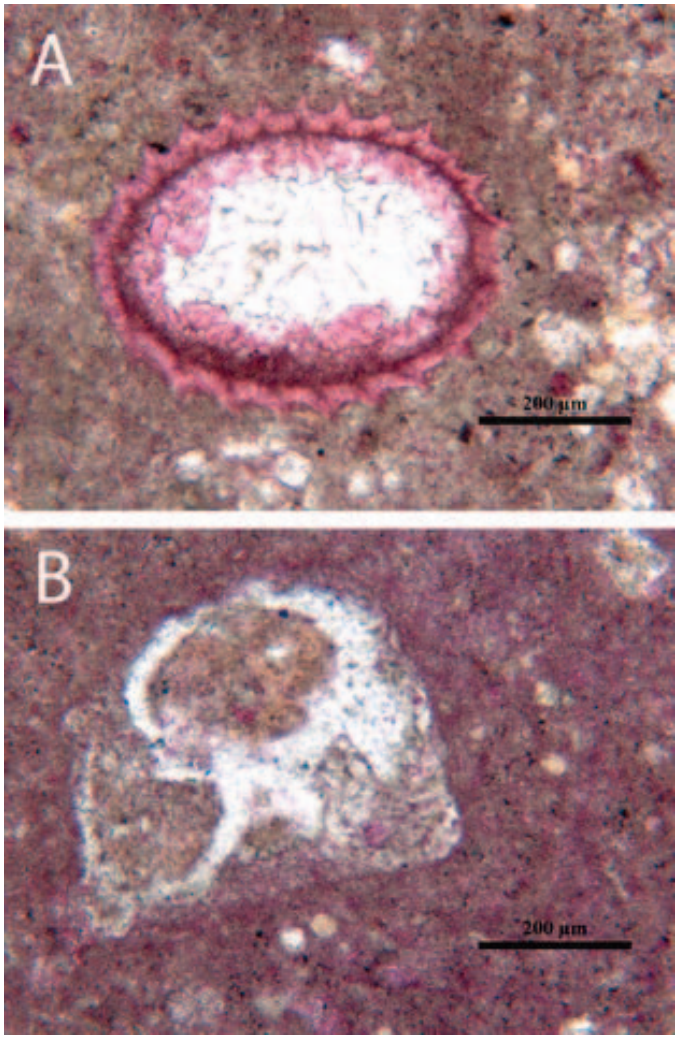

FIG. 6.—Middle Bed I. **A)** Photomicrograph of a stained thin section (Dickson 1966) showing quartz-rich silt in micrite matrix, with a *Chara* oogonium. The oogonium is lined with nonferroan calcite cement (stained pink) and a subsequent stage of nonferroan dolomite cement (clear crystals). **B)** Stained photomicrograph of a gastropod shell mold within silty micrite.

Geochemistry.—The ICP results show high concentrations of Mn (~ 1000–2400 ppm) with two low-Mn outliers, both from the same sample (Table 2, Fig. 7A). Strontium concentrations are variable (~ 320–2000 ppm) (Fig. 7B) with two high-value outliers from the same sample. Magnesium values are generally low except for two outliers, from the same sample with the high Sr (Fig. 7C), and iron values have a modest range (~ 300–3000 ppm) (Fig. 7B).

Stable Isotopes.—Samples from the Middle Bed I limestone have a considerable range in both oxygen and carbon isotope ratios (Fig. 8, Table 2). $\delta^{18}O$ values range from −5.27‰ to 0.08‰, with a mean of −3.11‰, and $\delta^{13}C$ values range from −4.76‰ to 2.79‰ with a mean of −1.22‰.

Upper Bed I

Depositional Characteristics.—This carbonate bed averages between 0.2 to 0.5 m thick, can be traced laterally for tens of meters, and locally forms a mound up to 1.4 m thick (Fig. 5B) (Ashley et al. 2010a; Baluyot 2011; Ashley et al. 2014). The outcrops are in close proximity to mapped faults. An airfall tuff (Tuff IF) blankets Upper Bed I, facilitating correlation between outcrops, and drapes over it, indicating original topographic mound relief. The Tuff is 1.803 ± 0.002 Ma (Deino 2012) and erupted from Olmoti in the Ngorongoro Volcanic Highland (Fig. 3) (McHenry et al. 2008; Stollhofen et al. 2008). The carbonate is porous micrite, with chalky textures, and is friable to moderately indurated with calcite spar and patchy secondary dolomite. One sample consists of well-indurated dolomite. The carbonate is light colored (white to tan) calcite, with spongy to nodular fabrics. Root casts, brown to yellow clay patches, and nodular to platy fabrics are common.

Petrographic Characteristics.—Ostracod shells, volcaniclastic rock fragments, and mineral grains occur in bioturbated, peloidal, non-ferroan micrite. Siliciclastic silt-size grains, such as pyroxene, biotite, and plagioclase feldspar, are angular to subangular. Rhizoconcretions and root molds are common (Fig. 9A).

Diagenetic Characteristics.—Rhizoconcretions and root molds, as well as shrinkage cracks and circumgranular cracks, are commonly associated with pyrolusite-rich rims (Fig. 9A). Cements include sparry nonferroan calcite and dolomite crystals within pores, dolomite being the last carbonate mineral to precipitate, based on sequential stages of cement generation (Fig. 9B). Partial fine-grained dolomitization of the micrite matrix occurs in most samples.

Geochemistry.—XRD results indicate calcite as the dominant carbonate mineral with minor dolomite (Table 1). Elemental analysis of the matrix shows relatively low levels of Sr (279–633 ppm), with five samples containing > 900 ppm Sr (Fig. 7A), modest levels of Mg (~ 2500–48,000 ppm), but a wide range in Fe (Fig. 7B). Although many samples contain less than 1000 ppm Fe^{2+}, others range up to 6787 ppm Fe^{2+}. Mn clusters between 47 ppm and 226 ppm, with four samples containing between 470 and 985 ppm Mn (Fig. 7A).

Stable Isotopes.—The carbonates have a range in $\delta^{18}O$ from −5.78‰ to −3.78‰, and the $\delta^{13}C$ values range from −5.57‰ to −1.83‰ (Fig. 8) (Baluyot 2011). The mean oxygen isotope value is −4.91‰, and the mean carbon isotope value is −3.67‰.

Upper Bed II

Depositional Characteristics.—The carbonate in this unit is ~ 1 m thick and can be traced laterally for over a kilometer along the south margin of the Side Gorge (Fig. 3). The locality is called BK (Leakey 1971). An identical bed at the same elevation occurs on the north side of the Side Gorge (called SC). The carbonate occurs above Tuff IID, which is dated to be ~ 1.2 Ma (Leakey 1971; Hay 1976) to 1.34 Ma (Domínguez-Rodrigo et al. 2013) (Fig. 4). The limestone is underlain at both sites (BK and SC) with a meter- thick bed that fines upward from silt to siliceous silty clay (with root casts) (Fig. 5C) and is overlain by green smectitic clay. The carbonate is typically porous but generally well indurated. At the west end of the BK outcrop, the rock is a creamy white micrite, but it gradually changes to brownish nodular chalky carbonate at the eastern end. At the SC site it is composed of brownish friable micrite.

Petrographic Characteristics.—The matrix in Upper Bed II is characterized by peloidal micrite containing ostracod carapaces (Fig. 10A), rhizoconcretions, and root molds. The siliciclastic component consists of angular volcaniclastic rock fragments, feldspar and quartz sand grains, and silt-size quartz grains.

TABLE 1.—*XRD mineralogy of carbonate units, Olduvai Gorge, Tanzania.*

Middle Bed I		Upper Bed I		Bed II	
GA-25-08	calcite 91% dolomite 9%	GA-13-07 *FLK-01*	calcite	GA-82-09	amorphous
GA-26-08	calcite	GA-17-07 *FLK-01*	calcite	GA-108-09 *spring head*	dolomite 99%
GA-40-08	calcite ferroan dolomite	GA-45-07 *FLK-01*	calcite	GA-110-09	calcite 79% dolomite 29%
GA-87·08	calcite (aragonite)	GA-46-07 *FLK-01*	calcite	GA-120-09	dolomite 99%
		GA-47-07 *FLK-01*	calcite	GA-122-09 *Tufa top*	calcite 49% dolomite 51%
		GA-50-07 *FLK-02*	calcite	GA-127-09 *Middle of tufa*	dolomite 98% calcite 2%
		GA-52-07 *FLK-02*	calcite	GA-42-1 *BK-East*	calcite
		GA-72-08 *FLK-N-3*	calcite	GA-43-11 *BK-East*	calcite
		GA-73-08 *FLK-N-3*	calcite, dolomite	GA-44-11 *BK-East*	ferroan dolomite
		GA-15-09 *FLK-W*	calcite	GA-45-11 *BK-East*	calcite ferroan dolomite
		GA-18-09 *FLK-W*	calcite	GA-48-09 *BK-3*	calcite
		GA-21-09 *FLK-W*	calcite	GA-75-09 *BK-3*	calcite
		GA-54-09 *FLK-NW*	calcite	GA-76-09 *BK-3*	calcite minor dolomite
			calcite	GA-157-12 GA-158-12 *SC*	calcite

Diagenetic Characteristics.—Circumgranular cracks and shrinkage fractures, commonly associated with pyrolusite, are abundant (Fig. 10B). The micrite is moderately to well lithified, often by aggrading neomorphism, and nonferroan calcite, followed by nonferroan dolomite precipitation as later-stage diagenetic cement, authigenically precipitating in open pores. Fine-grained dolomite also patchily replaces micrite in many samples.

Geochemistry.—Calcite is the dominant mineral, but dolomite makes up to 50% of the carbonate in some samples (Table 1). The presence of abundant dolomite is confirmed by particularly high Mg^{2+}, up to $>$ 120,000 ppm concentrations (Fig. 7C). Sr^{2+} values are also relatively high, up to $\sim$ 5900 ppm (Fig. 7C). Bennett et al. (2012) report that carbonates from Upper Bed II contain a strontium-rich dolomite. The Fe^{2+} and Mn^{2+} are relatively low and tightly clustered with few outliers (Fig. 7A, B).

Stable Isotopes.—$\delta^{18}O$ isotopes range from -3.87‰ to 0.98‰, with a mean of -2.49‰ and $\delta^{13}C$ isotopes have values of -3.67‰ to 0.39‰, with a mean of -1.62‰ (Fig. 8) (Karis et al. 2012). There is no significant variation or trend in the isotope values for Upper Bed II carbonates.

INTERPRETATION AND DISCUSSION

Depositional Processes

The presence of fish bones, *Chara*, ostracods, and aquatic gastropods indicates that the three carbonate units represent sites of ponded surface water (Peck 1953; Tasch 1973; Monty and Hardie 1976; Brasier 1980) and did not form initially as soil calcrete. Each standing water body was likely shallow and small (tens to hundreds of meters in diameter). Each of the three carbonate horizons share commonalities such as peloidal micrite, faunal remains, burrows, angular siliciclastic detrital grains, and rhizoconcretion development. The micrite matrix indicates that the water was alkaline and supersaturated with respect to calcite. The peloidal character of the micrite is due to bioturbation and fecal-pellet production by an associated infauna (Platt 1989; Ashley et al. 2013). Abundant stem or root molds indicate the former presence of *in situ* vegetation (Esteban and Klappa 1983; Purvis and Wright 1991; Liutkus 2009). These features indicate that the waters associated with carbonate precipitation were fresh (non-hypersaline) and oxygenated, with minimal siliciclastic input, and abundant paleovegetation.

Based on the presence of aquatic fauna, flora, trace fossils, composition, and geographic extent, we interpret that the carbonate horizons in Middle Bed I, Upper Bed I, and Upper Bed II formed as in small bodies of standing or gently flowing water from springs or seeps, as discussed below. All of the limestones have distinct and localized geographic distributions, making them unlike paleo–Lake Olduvai lithologies, which are dominated by widespread waxy clays (magnesium-rich smectite), silts, and fine-grained sands that occur throughout Olduvai Basin (Hay 1976; Hay and Kyser 2001).

As noted by others (Tandon and Andrews 2001; Deocampo 2002; Liutkus and Ashley 2003), freshwater wetlands with associated carbonate deposits may contain a diverse flora and fauna, sustained by alkaline, mineral-enriched groundwater. Carbonate precipitation may be enhanced when CO_2-rich groundwater enters wetlands as seeps, or is released at faults (Ashley 2001; Ashley and Hay 2002).

Our geochemical results indicate that the groundwater feeding the carbonate depositional environments contained manganese, iron, strontium, and magnesium as dissolved constituents. In the Central Kenya Rift today, groundwater contains elements derived from volcanic bedrock (Olago et al. 2009). These authors describe local fracture systems that create multiple aquifers, with different groundwater recharge and discharge rates (Olago et al. 2009). Aquifers occur along weathered contacts between lava flows or fractured volcanic horizons. This plumbing system moves groundwater towards the Kenyan Rift rivers

TABLE 2.—*Elemental and stable-isotopic compositions.*

Middle Bed I			Upper Bed I			Upper Bed II			Upper Bed II cont'd		
Sample	$\delta^{18}O$ ‰	$\delta^{13}C$ ‰	Sample	$\delta^{18}O$ ‰	$\delta^{13}C$ ‰	Sample	$\delta^{18}O$ ‰	$\delta^{13}C$ ‰	Sample	$\delta^{18}O$ ‰	$\delta^{13}C$ ‰
GA-01-08	−3.40	−1.60	GA-15-07	−4.60	−2.80	GA-48-09A	−2.83	−1.92	GA-49-10	−2.21	−1.89
GA-02-08	−2.30	−1.70	GA-16-07	−4.90	−3.30	GA-48-09B	−2.99	−1.81	GA-50-10	−1.71	−1.58
GA-03-08	−3.00	0.40	GA-17-07	−5.30	−4.50	GA-48-09C	−2.29	−1.64	GA-25-11	−1.48	−1.17
GA-22-08	−3.73	−2.85	GA-27-07	−5.13	−3.39	GA-50-09A	−3.25	−1.18	GA-42-11	−2.81	−1.24
GA-24-08	−3.55	−2.13	GA-28-07	−4.56	−2.89	GA-50-09B	−3.21	−1.72	GA-43-11	−2.27	−1.08
GA-25-08	−3.63	−2.41	GA-29-07	−4.73	−3.53	GA-50-09C	−3.15	−1.83	GA-44-11	−1.06	−2.06
GA-26-08	−2.87	−2.07	GA-30-07	−4.55	−3.68	GA-75-09A	−2.73	−1.48	GA-45-11	−2.50	−1.61
GA-29-08	−2.02	−0.91	GA-31-07	−3.78	−1.83	GA-75-09B	−2.81	−1.35	GA-46-11	−2.19	−1.34
GA-30-08	−1.17	0.17	GA-32-07	−5.50	−4.16	GA-76-09A	−2.52	−1.18	GA-47-11	−2.52	−1.58
GA-31-08	−3.54	−2.45	GA-33-07	−5.05	−4.12	GA-76-09A	−2.45	−2.03	GA-48-11	−1.89	−1.68
GA-38-08	−2.09	−0.72	GA-34-07	−5.74	−5.90	GA-76-09C	−2.97	−1.20	GA-49-11	−2.13	−1.58
GA-39-08	−3.40	−2.64	GA-35-07	−5.25	−5.06	GA-107-09A	−2.13	−0.33	GA-52-11	−0.98	−0.67
GA-40-08	−3.54	−2.62	GA-45-07	−4.40	−2.00	GA-107-09B	−2.08	−0.53	GA-53-11	−3.65	−1.89
GA-46-08	−2.26	1.76	GA-46-07	−4.90	−3.20	GA-108-09	−1.46	−2.29	GA-21-12	−3.70	−1.69
GA-56-08	−3.84	−3.11	GA-47-07	−5.20	−4.20	GA-110-09	−2.17	−1.98	GA-22-12	−3.79	−2.46
GA-59-08	−4.34	−3.32	GA-50-07	−5.00	−3.70	GA-120-09	−1.75	−0.89	GA-25-12	−3.72	−2.34
GA-84-08	−3.70	−2.48	GA-51-07	−5.40	−4.40	GA122-09	−2.76	−1.87	GA-26-12A	−2.80	−1.81
GA-85-08	−3.12	−1.95	GA-52-07	−4.10	−2.10	GA-123-09A	−2.18	−0.13	GA-26-12B	−3.13	−1.85
GA-87-08	−5.03	−4.76	GA-53-07	−5.30	−3.70	GA-123-09B	−1.90	−0.23	GA-27-12A	−2.41	−1.71
GA-01-09	−4.62	−2.35	GA-54-07	−5.78	−5.32	GA-03-10	−2.66	−1.44	GA-27-12B	−1.92	−1.68
GA-03-09	−1.92	−1.28	GA-115-07	−4.50	−2.80	GA-04-10	−3.41	−1.99	GA-28-12A	−1.65	0.39
GA-15-09	−5.00	−2.67	GA-72-08	−4.20	−2.50	GA-05-10	−1.09	−1.44	GA-28-12B	−2.29	−1.95
GA-17-09	−3.11	−0.34	GA-73-08	−3.90	−2.50	GA-06-10	−2.94	−2.57	GA-29-12	−1.65	−2.16
GA-18-09	−2.51	1.00	GA-25-09	−5.17	−4.37	GA-15-10A	−1.77	−2.37	GA-31-12	−1.69	−2.14
GA-19-09	−3.18	0.34	GA-26-09	−5.14	−3.78	GA-15-10B	−1.98	−1.91	GA-32-12	−1.78	−1.57
GA-20-09	0.04	2.79	GA-27-09	−5.28	−4.27	GA-17-10	−3.88	−1.41	GA-35-12	−1.84	−2.33
GA-21-09	0.08	2.61	GA-28-09	−5.25	−4.54	GA-23-10	−2.84	−1.21	GA-130-12	−3.64	−2.82
GA-53-09	−4.90	−1.07	GA-29-09	−4.47	−2.64	GA-25-10	−2.83	−1.73	GA-131-12	−3.87	−3.67
GA-54-09	−5.27	−1.27	GA-30-09	−4.85	−3.37	GA-48-10	−3.79	−1.93			
GA-55-09	−2.61	0.85	GA-31-09	−5.48	−5.57						

Middle Bed I					Upper Bed I					Upper Bed II				
Sample	Mg ppm	Mn ppm	Sr ppm	Fe ppm	Sample	Mg ppm	Mn ppm	Sr ppm	Fe ppm	Sample	Mg ppm	Mn ppm	Sr ppm	Fe ppm
GA-25-08A	29093	1535	1949	3007	GA-15-07A	18393	155.8	588.0	1282.0	GA-48-09A	10698	360.0	1332.0	2357.0
GA-25-08B	15796	1038	1408	900	GA-15-07B	14576	101.2	482.6	871.5	GA-48-09B	7774	262.0	1396.0	991.0
GA-26-08A	14369	2113	1129	2813	GA-16-07A	48248	177.4	633.0	4141.0	GA-50-09A	1551	91.0	737.0	290.0
GA-26-08B	6214	2380	1165	3257	GA-16-07B	10061	84.5	394.0	384.1	GA-50-09B	6103	264.0	1393.0	1720.0
GA-40-08A	18704	1991	1272	2856	GA-17-07A	7660	144.8	501.9	151.7	GA-50-09C	33622	82.8	571.0	1966.0
GA-40-08B	7695	988	593	686	GA-17-07B	7517	222.7	542.8	144.7	GA-75-09A	9730	669.0	1445.0	1832.0
GA-87-08 A	5682	1160	563	2236	GA-17-07C	17157	226.3	1003.0	395.5	GA-75-09B	3054	301.0	910.0	339.0
GA-87-08B	3552	1720	415	519	GA-45-07A	24898	147.4	564.0	3475.0	GA-76-09A	3761	131.0	863.0	539.0
GA-87-08C	2226	1301	320	260	GA-45-07B	7215	120.0	335.0	713.0	GA-76-09B	6947	236.0	1172.0	1429.0
GA-01-09A	121290	264.2	5013	925	GA-46-07A	2973	59.0	279.0	96.0	GA-108-09A	115760	118.8	nd	787.0
GA-01-09B	80737	125	2595	312	GA-46-07B	15989	156.7	492.4	1120.0	GA-108-09B	121135	141.4	5815.0	339.9
					GA-47-07A	21338	123.0	603.0	770.0	GA-110-09A	68158	194.0	2815.0	737.0
					GA-47-07B	6613	165.0	590.0	120.0	GA-110-09B	74457	122.9	2784.0	276.9
					GA-50-07	11894	47.6	469.7	490.1	GA-110-09C	81302	181.7	3004.0	550.5
					GA-52-07A	8827	57.0	299.0	716.0	GA-120-09A	114955	54.1	5964.0	946.0
					GA-52-07B	38942	190.4	473.6	5959.0	GA-120-09B	68082	50.3	3427.0	703.3
					GA-52-07C	41484	203.9	471.7	6787.0	GA-120-09C	83801	56.8	3645.0	691.6
					GA-72-08A	16869	648.0	1014.0	4266.0	GA-122-09A	58898	157.2	2725.0	722.3
					GA-72-08B	16158	565.0	988.0	3344.0	GA-122-09B	127363	39.1	5813.0	419.9
					GA-73-08A	14906	613.0	2192.0	3741.0	GA-122-09C	74573	143.2	3490.0	1045.0
					GA-73-08B	13048	470.0	1744.0	1350.0	GA-42-11A	11070	345.0	2042.0	1911.0
										GA-42-11B	3153	115.0	982.0	252.0
										GA-43-11A	6967	269.0	1036.0	189.0
										GA-43-11B	5567	271.0	934.0	140.0
										GA-44-11A	94390	104.0	5398.0	425.0
										GA-44-11B	33869	32.0	2116.0	34.0
										GA-45-11A	20463	120.0	1353.0	125.0
										GA-45-11B	37384	237.0	2119.0	745.0
										GA-46-11A	31305	296.0	1592.0	1994.0
										GA-46-11B	10555	105.0	804.0	161.0
										GA-47-11A	13917	144.0	1086.0	131.0
										GA-47-11B	28215	291.0	2033.0	442.0

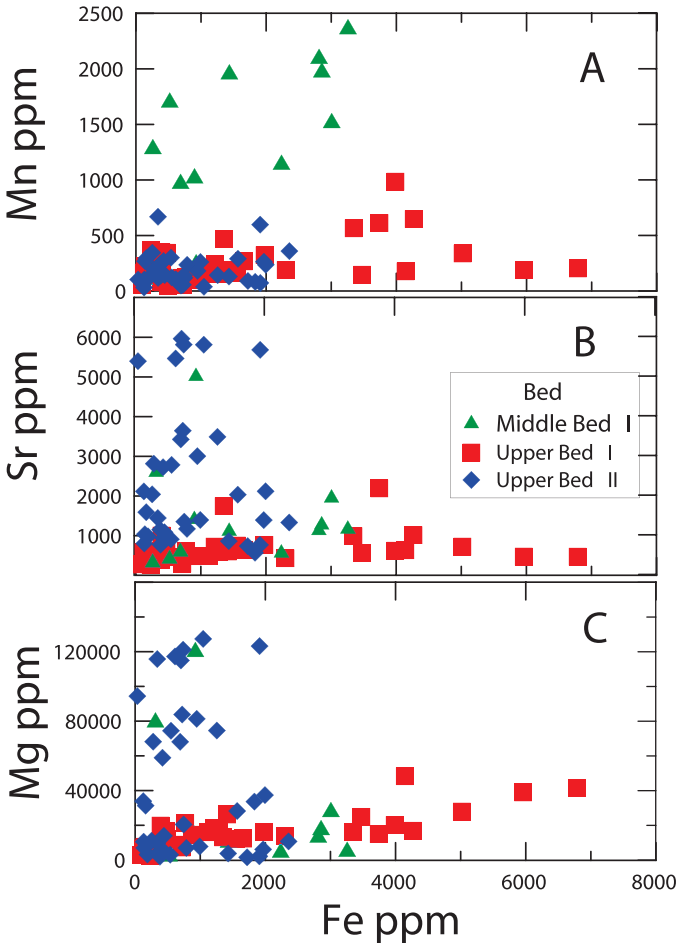

FIG. 7.—Element abundances (ppm) in limestone beds. **A)** Mn vs. Fe, **B)** Sr vs Fe, and **C)** Mg vs Fe, in ppm. Horizontal axes are the same, vertical axes vary with cation concentration. Limestones associated with fault zones (round symbols; Middle Bed I and Upper Bed I) are distinct from the carbonate associated with a groundwater-seep settings (diamonds; Upper Bed II). Limestone associated with the seeps have higher Sr and Mg concentrations due to the abundance of secondary Sr-rich dolomite in the micrite matrix. Volcanic-sourced groundwater, with enhanced water–rock interactions related to the fault system, produced carbonate with higher Fe and Mn values.

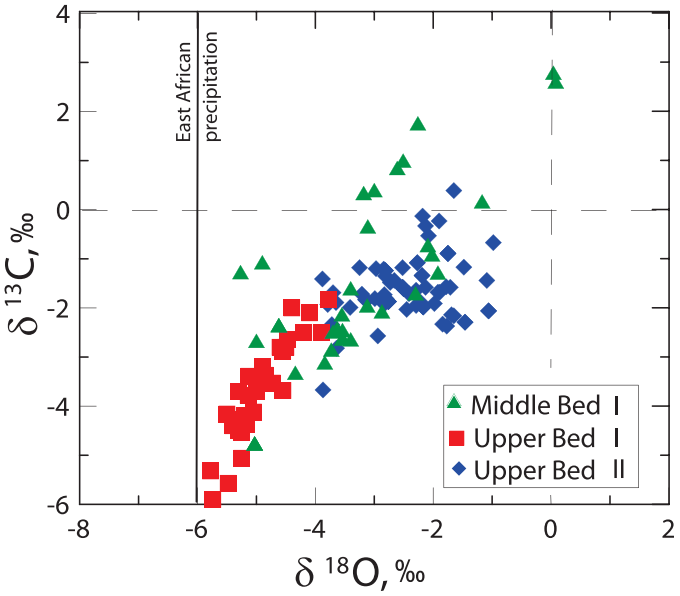

FIG. 8.—$\delta^{13}C$ and $\delta^{18}O$ ratios from the three limestone units. Upper Bed I carbonates have the lowest $\delta^{13}C$ and $\delta^{18}O$. Middle Bed I samples exhibit the broadest range in isotope ratios for both carbon and oxygen, and Upper Bed II samples have the highest.

and lakes at variable rates, but maintains Ca, Mg, Na, K, Cl, and F as major ions in the fluid (Olago et al. 2009). HCO_3 is the dominant anion, and both groundwater and surface waters are saturated with respect to Fe and Mn oxides and hydroxides are slightly undersaturated with respect to calcite and dolomite. Evaporation and soil–water–rock interactions concentrate ions to reach calcite and dolomite saturation in the modern lake waters, resulting in carbonate precipitation (Olago et al. 2009).

As in the Kenya Rift, volcaniclastic deposits and igneous rocks underlie, overlie, and occur in the immediate vicinity of the Olduvai limestones, meaning that they were readily available to be physically transported as clasts and mineral grains into carbonate-depositing seeps or springs, as we and others have noted (Hay and Reeder 1978; Hay and Kyser 2001; McHenry 2009; Mollel et al. 2009). It also means that volcanic-derived constituent elements were readily available as dissolved ions in the groundwater, and thus influenced limestone composition when the waters reached supersaturation at spring and seep sites. Studies elsewhere have noted that ash weathers readily and constituent ions are easily transported in solution (Quade et al. 1995). For example, Quade et al. (1995) found 10–20% of calcium in Australian soils is derived from regional volcanic material. Similarly, the presence of abundant dissolved ions, expressed as constituent elements in the Olduvai limestones, suggests that breakdown of regional igneous rocks provided a ready source of ions to the groundwater system. Mollel et al. (2009) report a range of oxides present in the volcanic materials associated with Bed I in Olduvai Gorge, including MnO, FeO, MgO, and CaO. One of the lavas has high MnO values (up to 4.1 wt%) (Mollel et al. 2009). McHenry (2009) reports that fluids moving down through the stack of Olduvai Gorge tuffs are enriched in multiple elements derived from breakdown of volcanic material. Thus, it appears that cations such as Mn, Fe, Mg, and Sr were readily available to be transported in the regional groundwater.

All three of the Olduvai limestones in our study contain pyrolusite concentrations in association with rhizoconcretions. This is similar to findings in a study from Lake Turkana in northern Kenya, where Mount and Cohen (1984) concluded that aquatic and nearshore vegetation appeared to concentrate Mn, triggering redox changes in the pore water. Reducing conditions developed as plant tannins were released into the water, lowering pH values. During very early diagenesis, suboxic to anoxic pore waters enable Mn to be converted to its divalent state and thus substitute for Ca in precipitating calcite (Mount and Cohen 1984). Mn^{2+} is particularly abundant in the micrite from Middle Bed I, as noted in our ICP results (Fig. 7A). Mount and Cohen (1984) describe a hundredfold increase in Mn in marginal lake sediments where plants are abundant, relative to open lake water. Other studies in modern (McCarthy and Ellery 1995) and ancient (Bustillo and Alonso-Zarza 2007) wetlands noted that aquatic vegetation is known to modify water chemistry. We suggest that a similar process of Mn enrichment due to biological concentration occurred in the Olduvai limestones, but particularly within Middle Bed I. Allan Pentecost noted that an association between Mn mineralization and depositional carbonate is known to occur in some springs (Pentecost 2005). Ashley et al. (2013) report that suboxic conditions within wetland sediments facilitate the Mn (and Fe) reduction to 2+ valence conditions. Because Mn is more readily reduced to its divalent state than is Fe, it is likely that even under suboxic conditions Mn would have been available as Mn^{2+} to substitute for Ca^{2+} in the Olduvai carbonates. The presence of ferrous-iron concentrations up

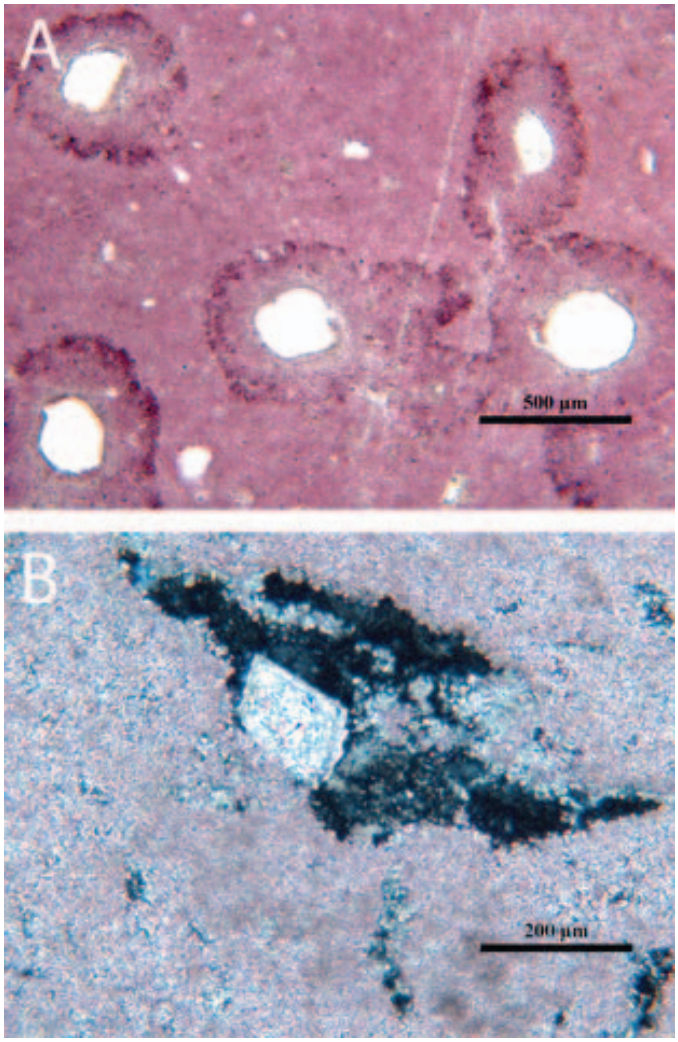

FIG. 9.—Upper Bed I. **A)** Photomicrograph of stained thin section showing pyrolusite-rich rims around rhizoconcretions or plant stem molds in peloidal micrite. The center of the stem molds is uncemented void space. **B)** Photomicrograph taken with crossed nicols showing a single dolomite rhomb precipitated within a shrinkage crack in non-ferroan, burrowed micrite.

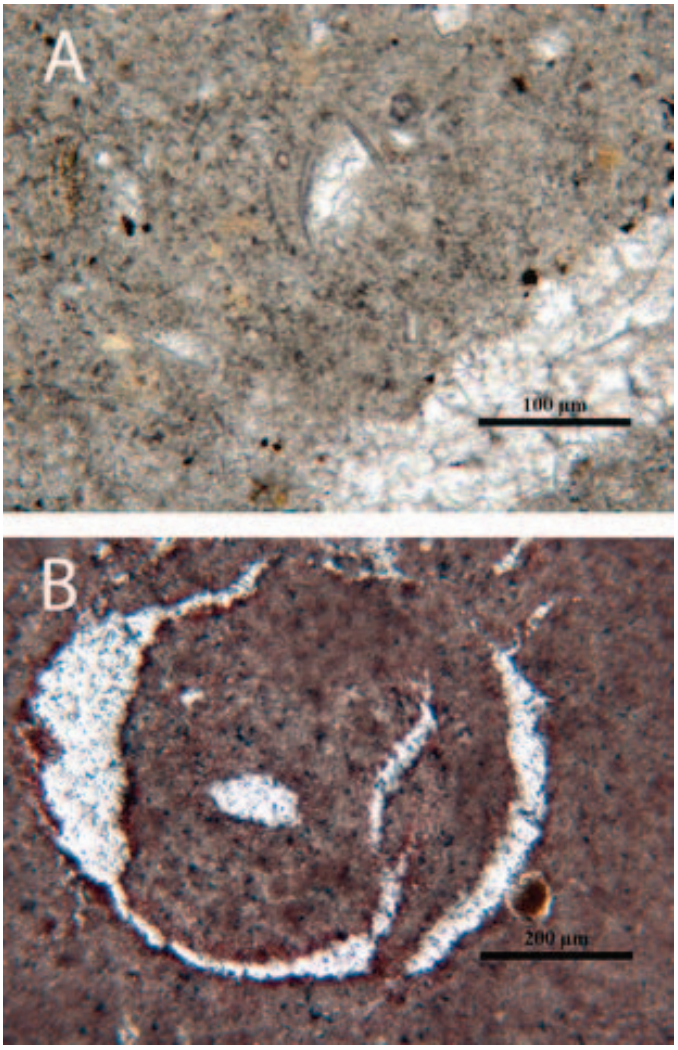

FIG. 10.—Upper Bed II. **A)** Photomicrograph of unstained thin section showing ostracod shell fragments in peloidal micrite with diagenetic calcite sparry cement. **B)** Photomicrograph of a stained thin section with bioturbated nodular micrite and circumgranular cracks due to pedogenesis.

to almost 7000 ppm in Upper Bed I micrite (Fig. 7B) indicates that pore waters did become anoxic at some point in time, facilitating iron substitution into the precipitating calcite.

These ions, dissolved in the groundwater, are expressed in the Olduvai limestones in different ways. Middle Bed I and Upper Bed I are enriched in either manganese (Middle Bed I) or iron (Upper Bed I), relative to the carbonate in Upper Bed II (Fig. 7). Upper Bed II (Fig. 7), however, is enriched in magnesium and strontium, relative to the other two limestone deposits. We suggest that Middle Bed I and Upper Bed I carbonates formed by a different mechanism than did Upper Bed II, as discussed below. Although the three limestones share many common features, they differ in a number of characteristics, leading to the following specific environmental interpretations.

Depositional Environments

Fault-Related Sites.—Middle Bed I has a mound-shaped form and is associated with the Zinj fracture system, as mapped in the field (Fig. 11A). The mound and fault system suggest a focused source for the water, likely a spring, flowing into a small pond or wetland, as can be observed in rift basins today (Olago et al. 2009). Although fieldwork does not show any faults directly leading to the limestone, mapping reveals numerous faults in the immediate area, and the $\delta^{18}O$ signature of the mound carbonate is quite negative, suggesting local and rapid calcite precipitation without evaporative fractionation (Fig. 8). In contrast, the $\delta^{18}O$ of the widespread but thin surrounding carbonate deposits in Middle Bed I are much more positive, indicating evaporation-induced change associated with delayed precipitation. Oxygen isotope ratios indicate that some evaporative fractionation may have occurred, as shown with the two samples that have the least negative oxygen isotope ratios (0.08, 0.04‰). Many samples have isotopic ratios more positive than the present-day meteoric-water ratio of −6‰ (VPDB equivalent to −4‰ VSMOW) (Bowen 2010). Although the mean for Middle Bed I oxygen isotope values is −3.11‰, some samples have values that are enriched in the lighter isotope, and may, therefore, reflect some surface water mixing with groundwater (Ashley and Hay 2002).

The geochemical data indicate that pore waters contained volcanic-sourced cations that were incorporated into precipitated calcite and dolomite; therefore, those same pore waters are likely to contain some

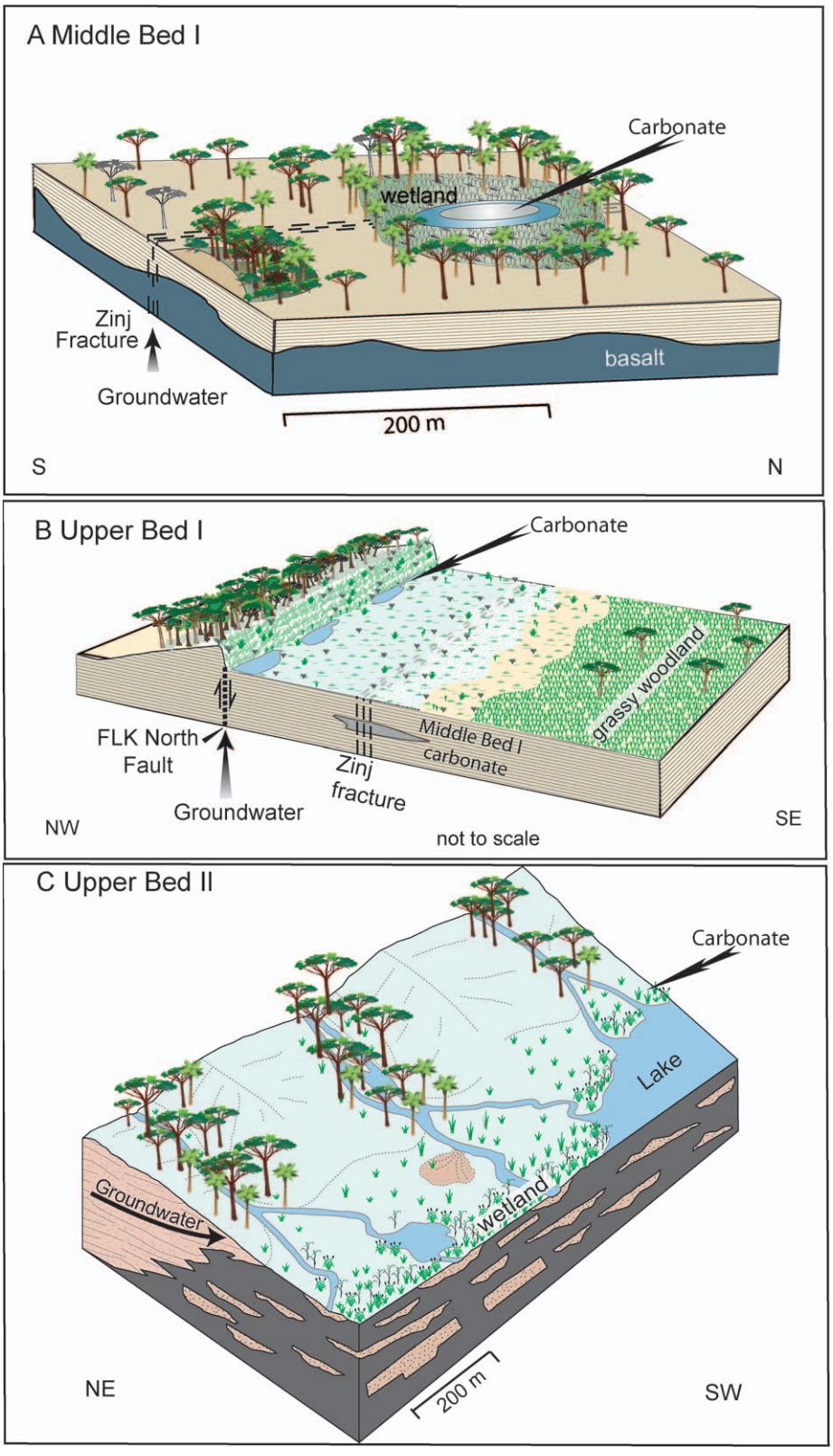

FIG. 11.—Depositional models. Diagrammatic reconstructions of the interpreted paleoenvironment of the three limestones. **A)** Middle Bed I limestone was sourced from groundwater emanating from a fracture (Zinj Fracture), creating a carbonate mound. Carbonate-precipitating wetland surrounded the mound. Vegetation distribution is from Ashley et al. (2010b). **B)** Upper Bed I limestone was sourced from groundwater flowing from a fault (FLK North Fault). A carbonate mound was formed by water flowing from the fault. Vegetation distribution is from Barboni et al. (2010). **C)** Upper Bed II limestone formed from seepage of groundwater at base of slope. The depositional environment is modelled after Arenas et al. (1997).

volcanic-derived oxygen as well. The wide range in oxygen values measured from Middle Bed I carbonates may reflect a number of oxygen sources, with certain sources or processes dominating seasonally or on a longer-term time scale. Carbon isotope ratios also exhibit the widest range, relative to Upper Bed I and Upper Bed II samples (−4.76 to 2.79‰). This range supports other geochemical evidence for a mix of fluid sources, in this case probably both volcanogenic CO_2 and CO_2 associated with plant respiration (Ashley and Hay 2002).

Collectively, the data from Middle Bed I indicate that groundwater, enriched with volcanic-derived cations, debouched from a fault-generated spring source and flowed into a small vegetated wetland. The carbonate-precipitation paludal wetland interpretation is supported by the presence of root casts, Charophyte oogonia, gastropods, and ostracods (Pedley 1990). Figure 11A is a diagrammatic reconstruction based on this study and a previous study involving an archaeological site and the associated vegetation (Ashley et al. 2010b). The reconstruction is consistent with Pla-Pueyo et al., who stated that paleo-wetlands must show evidence that hydrophytes (fossil plants) were present (Pla-Pueyo et al. 2009). Stewart (1996) observed that fish inhabit small ponds and wetlands in rift basins during annual wet seasons, but often become stranded as the rains cease and intense seasonal evaporation begins. Leakey (1971) and Stewart (1996) interpreted the abundant fish bones in Middle Bed I as a death assemblage associated with seasonal drying conditions.

Carbon and oxygen stable-isotope signatures indicate a range of conditions for carbonate precipitation, with more negative values produced proximal to the presumed water source, the Zinj fracture, from more rapidly flowing groundwater, whereas the carbonate that precipitated in a more distal location from the Zinj fracture had more time to interact with the atmosphere and experienced higher levels of evaporation. Petrographic evidence from distal-site samples, such as shrinkage cracks, shows that the distal areas experienced a greater degree of pedogenesis associated with early diagenesis than limestones near the Zinj fracture, but in both areas, similar carbonate cements precipitated during shallow burial (secondary calcite and dolomite).

Upper Bed I is also interpreted to have formed from groundwater flowing from a fault, in this case the FLK North fault (Fig. 11B). The localized, mound-shaped form of the limestone (Fig. 5B) indicates a narrow source of groundwater discharge. Barboni et al.'s (2010) analysis of phytoliths from Upper Bed I indicates locally dense and heterogeneous paleovegetation associated with freshwater springs. The presence of plants is supported by our petrography showing abundant rhizoconcretions in the Upper Bed I micrite. Upper Bed I is characterized by high Fe^{2+} concentrations, tightly clustered Sr^{2+} values, covariant stable isotopes that are depleted relative to Middle Bed I and Upper Bed II, and field evidence for an association with local faults (mound-like form and local faults have calcite infilling).

We interpret that Upper Bed I carbonates formed mainly from reducing groundwater as it debouched along fault conduits (Hay et al. 1986; Pedley et al. 1996; Mack et al. 2000; Kampman et al. 2012) (Fig. 11B). The normal-fault interpretation in Figure 11B is from Ashley et al. (2010a) and vegetative cover from Barboni et al. (2010). The fluid had a relatively homogeneous groundwater source as evidenced by the tight cluster of isotope ratios derived from the carbonates. Stable-isotope ratios from Upper Bed I limestones exhibit strong covariation. Talbot (1990) and Bustillo and Alonso-Zarza (2007) suggest that covariation may reflect closed conditions where isotope fractionation is relatively limited in its scope. Based on our results, Upper Bed I limestones formed as localized spring deposits where reducing, CO_2-rich groundwater was released at the surface. The rapid release of CO_2 lead to carbonate precipitation with tightly clustered isotope ratios reflecting a relatively homogeneous fluid composition (Mack et al. 2000), compared with the wetland carbonates stratigraphically below and above it (Middle Bed I and Upper Bed II). Covariant trends, such as exhibited by the Upper Bed I carbonates, may reflect closed conditions (Talbot 1990).

Oxygen isotope values obtained from Upper Bed I limestones are the most negative of the three horizons studied, indicating the least overall evaporation, and also suggestive of slight warming of the pore fluids while in the groundwater and fault system (Mack et al. 2000). In Spain, a study interpreting similar types of limestone suggests that a tight clustering of $\delta^{18}O$ values may represent a meteoric-water source (Alonso-Zarza et al. 2012). Upper Bed I Olduvai limestones exhibit a narrow range of oxygen isotope values, suggesting that the water was derived directly from a fault-related phreatic plumbing system sourced by meteoric water. Megafauna-bone evidence from a nearby archaeological site, FLK North, suggests that animals found this water potable (Leakey 1971; Domínguez-Rodrigo and Barba 2007; Bunn et al. 2010). Therefore, it is likely that hominids did as well, as supported by evidence of stone tools in the area around the seeps and springs (Domínguez-Rodrigo et al. 2010; Ashley et al. 2014).

We interpret that in the Olduvai Basin the carbonates in Middle Bed I and Upper Bed I were the records of discharge sites for groundwater associated with faults (Fig. 11A, B), similarly to the modern fracture system documented by Olago et al. (2009) in Kenya. The fault-related carbonates acquired additional Mn and Fe if their host waters drew on potentially deeper groundwater sources tapped by the fracture system, relative to shallow groundwater aquifers. Water moving through the deeper fault system likely meant longer travel time from the Ngorongoro Highland recharge area out into the Olduvai Basin, compared to shallow groundwater flow. Longer flow times provide increasing likelihood of water–rock interactions and element mobilization from the volcanics into the porewaters. In the Olduvai system, processes of groundwater degassing, evaporation, and water–rock interactions within the faults, coupled with paleovegetation, likely enhanced carbonate saturation and precipitation near springs. Fine-grained micrite and rhizoconcretions preserved in the stratigraphic succession record the shallow, vegetated wetlands associated groundwater discharge.

Seep-Related Sites.—Two seep-related sites were identified in the basin: Upper Bed II (Limestone #3) is included in this paper; Limestone #4 in Middle Bed I is newly discovered, and analyses will not be discussed here. Field relations indicate that the Upper Bed II limestone formed from groundwater seepage along a 1 km+ interface between the volcaniclastic fluvial plain (to east and south) and the paleo–Olduvai River valley (to the west), as shown in Figure 11C. Abundant rhizoconcretions and root molds occur and indicate significant paleovegetation. In addition, the occurrence of ostracod fossils suggests standing, or gently flowing water, rather than a soil. These occurrences resemble those in Middle Bed I and Upper Bed I fault-related limestones. The occurrence of ostrocodes and peloidal nature of the micrite, indicative of an active infauna, suggest that the water body was oxygenated, and the abundance of rhizoconcretions, indicating rooted vegetation suggests shallow water.

The thin, widespread geographic extent of this unit indicates a different depositional environment, contrasting with the mounded and localized carbonate in Middle Bed I and Upper Bed I. This Upper Bed II unit is closer to the edge of the basin, compared to Middle Bed I and Upper Bed I, which occur towards the basin center. We propose an environmental reconstruction of a distal fluvial plain, similar to examples from the Ebro Basin, Spain (Arenas et al. 1997) Geochemically, this unit is distinct from Middle Bed I and Upper Bed I. It is enriched in Mg and Sr and depleted in Fe and Mn, relative to the fault-related carbonates. Potentially, groundwater moving through unconsolidated alluvium on the Ngorongoro Highland alluvial-fan complex may have traveled relatively rapidly, with less water–rock interaction, reducing concentrations of Mn and Fe in the porewater. Magnesium and strontium values are related to secondary dolomitization; see Diagenesis section below.

The isotope ratios are relatively tightly clustered, with little variability. These differences lead us to interpret Upper Bed II carbonate as having formed at a localized seep (or multiple seeps) along the margin of a small playa lake or pond (Fig. 3). The groundwater drained from the highlands, as occurs today in Obalbal swamp at the edge of the present-day alluvial fan adjacent to the Ngorongoro Highland (Fig. 3). During the deposition of Upper Bed II, the Ngorongoro Highland was higher than it is today, potentially driving groundwater farther into the basin due to greater hydraulic head, debouching at the Upper Bed II locality. The isotope data

shows a modest (if any) evaporative trend and instead has fairly constant carbon isotopes (−2 ± 1‰). This flat trend may be consistent with vegetation controlled buffering of isotope exchange between organic material and the water and carbonate rather than evaporation control. Modern East African precipitation has a $\delta^{18}O$ of −4.0‰ VSMOW (Cerling and Quade 1993; Bowen 2010) (Fig. 8). It was likely the same in the past, but taking effects of mean annual temperature (~ 25 °C) into account, calcite precipitated under these conditions will have $\delta^{18}O$ (VPDB) equivalent values of −6‰. The mean of −2.49‰ in Upper Bed II indicates an open system of water flowing through the playa or pond under evaporative conditions such that oxygen isotope ratios reflect fractionation to be more positive than today's rainfall. We interpret this unit to have formed in a shallow, widespread, groundwater-fed wetland at the margin of a large pond (or paleo–Lake Olduvai when it was much reduced in extent) (Figs. 3, 11C), similar to other continental limestones reported elsewhere (McCarthy and Ellery 1995; Valero Garcés et al. 2008).

Diagenesis

We separated depositional characteristics from pedogenic features, characterizing pedogenesis as a very early diagenetic process. It is, however, difficult to delineate boundaries between depositional and early diagenetic processes (Freytet and Plaziat 1982; Alonso-Zarza 2003; Alonso-Zarza and Wright 2010). Armenteros et al. (1995) describe superimposed sedimentary–pedogenic associations from Miocene continental limestones in northern Spain, and another study in Argentina notes that authigenic minerals form very rapidly and may span both depositional and pedogenic regimes (Cabaleri and Benavente 2013). In the Olduvai limestones, pedogenesis is expressed through circumgranular, shrinkage, and desiccation cracking and nodular calcite cementation (Fig. 10B). Although pedogenesis may modify isotope ratios (Michel et al. 2013), each of the Olduvai carbonates studied here retain isotope signatures that differentiate them (Fig. 8), indicating a minimum amount of resetting through diagenetic soil-related processes.

Diagenesis took a similar pathway in each of the Olduvai carbonate horizons. Initially, pedogenesis produced changes in carbonate textures and growth of calcite cements (vadose and phreatic sparry calcite, micrite to microspar), resulting in a palustrine facies, *sensu* Freytet and Plaziat, without significant resetting of geochemical or isotope signatures (Freytet and Plaziat 1982). The sediment was physically modified as the site dried out, resulting in shrinkage cracks associated with subaerial desiccation, and calcite spar precipitation associated with vadose and phreatic meteoric waters (Platt 1989; Tandon and Friend 1989; Bustillo and Alonso-Zarza 2007). Purvis and Wright (1991) suggest that subhorizontal cemented beds containing rhizoconcretions and molds represent the location of a former water table, and that induration of shallow freshwater sediments may occur without significant burial, as shown in Quaternary wetlands from Spain (Alonso-Zarza et al. 2006). Middle Bed I, Upper Bed I, and Upper Bed II suggest a similar diagenetic history, where early lithification by calcite spar, derived from meteoric vadose and phreatic water, created subhorizontal cemented horizons without significant burial. Petrographic pedogenic textures in the Olduvai limestones are similar to those reported by Alonso-Zarza et al. (2006) and are similarly interpreted as having formed through episodes of wetting and drying, producing circumgranular cracks and mudcracks, with early lithification by vadose and phreatic calcite spar, without significant overburden or burial.

Subsequent burial by sediment from a phase of paleo–Lake Olduvai expansion likely facilitated further meteoric phreatic diagenesis in Middle Bed I, resulting in microspar and additional sparry calcite precipitation. Lake Cycle 1 (expansion and contraction) occurred after the deposition of Middle Bed I limestone and Tuff IC (Ashley 2007; Magill et al. 2012a) (Fig. 2). Diagenesis continued during burial under additional cycles of paleo–Lake Olduvai expansion, as the lake deposited clays, silts, and sandy sediments over the limestones (Hay and Kyser 2001). Petrographically, all three Olduvai limestones contain secondary dolomite as micrite replacement and pore-filling crystals, and our ICP data shows Mg in all samples. High Mg concentrations, particularly in Upper Bed II, reflect incorporation of late-stage dolomite.

Our ICP results show that Upper Bed II carbonate has high Sr values that covary with high Mg concentrations, supporting Bennett et al.'s (2012) report of high-Sr dolomite in Upper Bed II deposits. They suggest the dolomite formed in association with paleo–Lake Olduvai contraction and evaporative concentration. Hay and Kyser (2001) document dolostone layers within paleo–Lake Olduvai strata and state that the dolomite formed from dilute pore fluids associated with lake expansion. Precession-driven lake fluctuations meant that during wet periods, with lake expansion, lake water covered all of the limestone sites in our study (Ashley and Hay 2002; Magill et al. 2012b) (Fig. 3). Lake expansion would have allowed saline-lake and alkaline-lake brines to seep down through the limestones (Hay and Kyser 2001; Deocampo et al. 2009; McHenry 2009), partially dolomitizing the host micrite and producing dolomite in cavities, particularly when lake evaporation concentrated the descending pore fluids. Hay et al. (1986) and Hay and Kyser (2001) suggest that stable-isotope ratios from dolostone occurrences may reflect a single replacement dolomitizing event whereby Mg-enriched pore fluids altered primary calcific sand-size crystals to dolomite. Hay et al. (1986) note that diagenetic dolomite may retain approximately the same isotope values as the carbonate it is replacing or cementing if the system is closed. Paleo–Lake Olduvai was a closed system.

Dolomitization in continental settings, similar to the model proposed in this study, has been documented from a number of studies of sediments exposed to transient groundwater–lake water interactions, for example, in Israel (Hurwitz et al. 2000), in France (Colson and Cojan 1996), and in Spain (Bustillo and Alonso-Zarza 2007). In contrast, Hay et al. (1986) documented dolomitization of carbonate spring deposits during evaporative concentration of lake waters in Pliocene limestones, Amargosa Desert, USA. Groundwater may obtain supersaturation with respect to dolomite, and, therefore, precipitate diagenetic dolomite that might be difficult to distinguish from lake-water-derived dolomite (Khalaf 1990; Spötl and Wright 1992; Armenteros et al. 1995; Bustillo and Alonso-Zarza 2007), but in the Olduvai limestones the dolomite is secondary and is, therefore, a diagenetic phase related to postdepositional fluid migration.

Depositional Model: a Goldilocks Effect

The presence of freshwater limestone in the persistently arid Olduvai Basin raises some interesting questions. Why were there some time periods when carbonates precipitated, and other times when siliciclastic deposition dominated? Weathering of trachytic volcanic source rocks presumably consistently supplied abundant ions (including Ca^{+2}) to the basin, and the basin's internal drainage confined surface and groundwater within a relatively closed system throughout the last two million years. However, at certain times, limestones formed and conditions persisted for long enough to create meter-thick deposits. As observed by others, terrestrial carbonates represent climate periods when conditions are neither too wet nor too dry (Gasse et al. 1987; Gasse 1990; Ford and Pedley 1996; Kazancl et al. 1995). If conditions are too wet, then large amounts of siliciclastic debris will likely be eroded and transported in large-scale fluvial and lacustrine systems dominated by sands, silts, and clays (Dean and Fouch 1982; Suchecki et al. 1988). At Olduvai during very wet portions of the precession cycle the lake occupied most of the basin floor (Fig. 4). On the other hand, if conditions are too dry, there will be a paucity of surface and ground water to transport ions or allow significant accumulation beyond calcrete formation. Limited aquifer recharge,

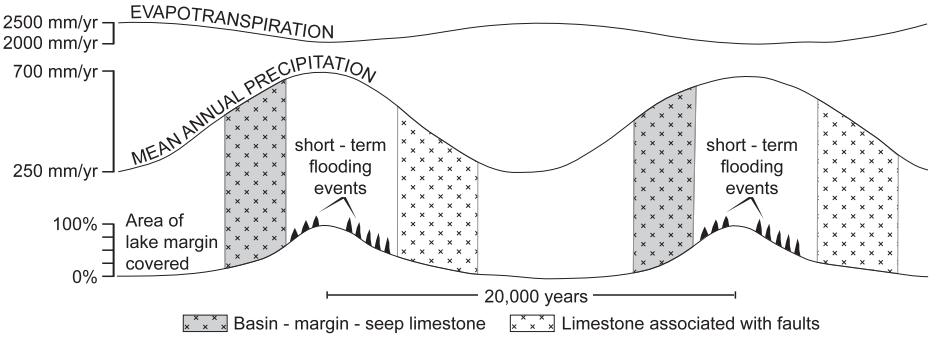

FIG. 12.—The Goldilocks Effect. A generalized model for the formation of freshwater limestone in arid rift basins is proposed. Time represented is 40,000 years (two precession cycles). The bottom curve traces the changing percent area of the lake margin flat that is covered and uncovered by the expanding and contracting lake. The middle curve shows the increase and decrease of mean annual precipitation as modulated by the precession orbital cycle. The top curve tracks the change in potential evapotranspiration that would increase and decrease slightly, out of phase with the wet/dry precession cycle.

coupled with low ion concentrations, will restrict carbonate formation in any appreciable amount (Dean and Fouch 1982; Gasse 1990). It seems that conditions for the development of reasonably thick (0.5–1 m) freshwater limestones in arid to hyperarid setting have to be just right, thus we use the term "Goldilocks Effect." In actual fact, semiarid climate conditions may be optimal for continental carbonate accumulation, as noted from central Namibia (Mees 2002) and in Cretaceous through Holocene limestone settings in Spain (Platt 1989; Ford and Pedley 1996; Alonso-Zarza et al. 2006; Bustillo and Alonso-Zarza 2007; Alonso-Zarza et al. 2012) Deep-water lakes indicate an overall positive water balance, but shallow lacustrine–palustrine facies imply a transitional state, where positive to negative water balances fluctuate across a narrow gradient and change readily from one state to another (Katz 1990; Ashley et al. 2013).

The Olduvai limestones occur in two distinct geographic contexts: basin-margin settings, where groundwater seeps out at base of slope, and fault-related settings, where faults act as conduits for groundwater. However, superimposed on these geographic setting is climate, which due to astronomic forcing is continuously changing on a time scale of ~ 20,000 years (Figs. 3, 4). Olduvai's hydrologic budget fluctuated during the precession cycle, as rainfall (P) increased and decreased, and potential evapotranspiration (PET) fluctuated, but was of lower amplitude, and out of phase with the precipitation (Fig. 12). Increased cloud cover, decreases in temperature, and increases in vegetation density will modulate the PET. However, during wet portions of the precession cycle, during lake expansion, lake-margin flat areas would be substantially reduced, covered by the expanding lake, and thus unavailable for palustrine deposition except in a narrow band up against the alluvial fan and the Ngorongoro Highlands to the east.

Because of decades of fine-scale stratigraphic analysis, coupled with precise age determinations on interbedded tuffs, Olduvai Gorge is an excellent place to test our model of the Goldilocks Effect for limestone deposition in arid terrigenous basins (Fig. 12). Figure 12 depicts the fluctuation of mean annual precipitation over a 20,000 year precession cycle, as modulated by astronomic forcing. The area of lake margin covered by water from paleo–Lake Olduvai is displayed as the lowermost curve. Because paleo–Lake Olduvai was always relatively shallow, it was highly responsive to precipitation fluctuations. In this case, wet and dry periods were more a function of flooding frequency than full vs. empty periods. Wet periods resulted in more frequent flooding, and dry periods reduced flooding frequency. It is, therefore, reasonable to assume that at 50% of the precession cycle the lake basin margin and floor were subaerially exposed, and exposure is required for the development of palustrine limestones. To form nonlacustrine limestones requires both available land surface, not covered in lake water, and a sufficient water supply. The groundwater flow to Limestones #1 and #2 followed direct flow paths to the surface through fracture or fault conduits (Fig. 11A, B), with aquifer recharge occurring during annual wet seasons. So the ideal conditions for limestone-precipitation sites situated on the basin floor are on the dry end of the wet-to-dry limb of the climate cycle (Figs. 4, 12).

However, Limestone #3 (Upper Bed II) formed under different geographic and climatic conditions. This depositional environment is a basin-margin seep, with no fault involved. The groundwater flow path is from the Mt Lemagurut to the base of slope at the edge of a small lake or large pond (Fig. 3). Because of the high PET, there was a narrow window of time when the groundwater discharge was sufficient to maintain a carbonate-precipitating wetland before the local water body floods the site. This window of time appears to have been during the rising limb of the climate cycle, but not at its maximum (Fig. 12). The Upper Bed II limestone is overlain by lake clays, suggesting that the wetland was flooded and buried by a subsequent phase of lake expansion (Ashley 2012; G.M. Ashley, unpublished data).

CONCLUSIONS

The limestone deposits in the Olduvai Basin are enigmatic, in that low rainfall and high potential evapotranspiration produce a persistent negative hydrologic balance. Previous studies have documented precession-controlled climate cycles during the early history of basin infilling, and the intercalated volcanics are well dated. This established chronology of climate change provides an ideal setting to determine the conditions of formation of the limestones which commonly occur associated with archeological sites including hominin remains. Petrographic analysis coupled with elemental and stable-isotope geochemistry indicates that the limestones were formed by precipitation of calcite from fresh groundwater flowing directly from faults or from seeps, both with associated vegetated wetlands. The carbonates formed periodically when the paleoenvironmental and paleoclimatic conditions were just right, i.e., a Goldilocks Effect. The conditions include a hydrogeologic setting with groundwater flow greater than evaporative loss under prevailing climatic conditions. The limestones formed under two climatic scenarios: wet-to-dry conditions (#1, Middle Bed I and #2, Upper Bed I) and dry-to-wet conditions (#3, Upper Bed II) and the newly discovered #4, Middle Bed I. The limestones also formed in two different hydrogeologic settings: (1) groundwater discharging from faults (#1, #2) or (2) slope margin seepage (#3, #4). Limestones deposited during drier portions of the precession cycle (falling limb) appear to be limited to groundwater discharge near faults. The groundwater, driven by hydraulic head and protected from evaporation, discharged onto dry lake flats. At maximum precipitation (peak of precession cycle), the area would have been flooded by the lake, inhibiting wetlands (Fig. 12). Limestones deposited during wetter times of the precession cycle (rising limb) occur in wetlands at the base of the slope. These fringing wetlands maintained by robust groundwater seepage were ultimately flooded out with rising lake level. A generalized model of limestone formation in arid rift basins is proposed using the climatic conditions determined in this study. However, the size, geology (volcaniclastic infill, extension tectonics, and presence of faults), and aridity of the Olduvai Basin are similar to many other continental rift sites around the world; thus the proposed model for freshwater limestone

forming in association with the rising and falling limbs of Milankovitch climate cycles may be applicable to numerous other locations.

ACKNOWLEDGMENTS

The raw data presented here were collected under permits from the Tanzania Commission for Science and Technology and the Tanzanian Antiquities Department to TOPPP (The Olduvai Paleoanthropology and Paleoecology Project), Principal Investigators M. Domínguez-Rodrigo, H.T. Bunn, A.Z.P. Mabulla, and E. Baquedano. We appreciate funding provided by the Spanish Ministry of Education and Science through the European project I+D HUM2007-6381507-63815 and the Ministry of Culture through funding to archeological research abroad. We are grateful to James Wright and Richard Mortlock for the stable-isotope analyses at Rutgers and to Steve Sylvester for XRD and ICP assistance at Franklin & Marshall College. Appreciation is extended to Jeremy Delaney for assistance with drafting figures. We thank associate editor Bruce Wilkinson and reviewer Jeff Pietras and an anonymous reviewer for their constructive comments that improved the manuscript. We also thank Vicki Pedone for her insights. All of us are indebted to the late R.L. Hay for his immense knowledge of the geology of Olduvai Gorge and his generosity in sharing his wisdom during many seasons in the field with GMA.

REFERENCES

Alonso-Zarza, A., 2003, Paleoenvironmental significance of palustrine carbonates and calcretes in the geological record: Earth-Science Reviews, v. 60, p. 261–298.

Alonso-Zarza, A.M., and Wright, V.P., 2010, Palustrine Carbonates, *in* Alonso-Zarza, A.M., and Tanner, L.H., eds., Carbonates in Continental Settings: Facies, Environments and Processes: Amsterdam, Elsevier, Developments in Sedimentology, no. 61, p. 103–131.

Alonso-Zarza, A.M., Dorado-Valiño, M., Valdeolmillos-Rodríquez, A., and Ruiz-Zapata, M.B., 2006, A recent analogue for palustrine carbonate environments: the Quaternary deposits of Las Tables de Daimiel wetlands, Cuidad Real, Spain, *in* Alonso-Zara, A.M., and Tanner, L.H., eds., Paleoenvironmental Record and Applications of Calcretes and Palustrine Carbonates: Geological Society of America, Special Paper 416, p. 153–168.

Alonso-Zarza, A.M., Meléndez, A., Martin-Garcia, R., Herrero, M.J., and Martín-Pérez, A., 2012, Discriminating between tectonism and climate signatures in palustrine deposits: lessons from the Miocene of the Teruel Graben, NE Spain: Earth-Sciences Reviews, v. 113, p. 141–160.

Arenas, C., Casanova, J., and Pardo, G., 1997, Stable-isotope characterization of the Miocene lacustrine systems of Los Monegros (Ebro Basin, Spain): palaeogeographic and palaeoclimate implications: Palaeogeography, Palaeoclimatology, Palaeoecology, v. 128, p. 133–155.

Armenteros, I., Angeles Bustillo, M.A., and Blanco, J.A., 1995, Pedogenic and groundwater processes in a closed Miocene basin (northern Spain): Sedimentary Geology, v. 99, p. 17–36.

Ashley, G.M., 2001, Archaeological sediments in springs and wetlands, *in* Stein, J.K., and Farrand, W.R., eds., Sediments in Archaeological Contexts: Salt Lake City, University of Utah Press, p. 183–210.

Ashley, G.M., 2007, Orbital rhythms, monsoons, and playa lake response, Olduvai Basin, equatorial East Africa (~ 1.85–1.75): Geology, v. 35, p. 1091–1094.

Ashley, G.M., 2012, A groundwater-fed mega wetland: a perennial source of water for hominins, Upper Bed II, Olduvai Gorge, Tanzania [abstract]: Geological Society of America, Abstracts with Programs, v. 44, p. 358.

Ashley, G.M., and Hay, R.L., 2002, Sedimentation patterns in an Plio-Pleistocene volcaniclastic rift-margin basin, Olduvai Gorge, Tanzania, *in* Renaut, R.W., and Ashley, G.M., eds., Sedimentation in Continental Rifts: SEPM, Special Publication 73, p. 107–122.

Ashley, G.M., Tactikos, J.C., and Owen, R.B., 2009, Hominin use of springs and wetlands: paleoclimate and archaeological records from Olduvai Gorge (1.79–174 Ma): Palaeogeography, Palaeoclimatology, Palaeoecology, v. 272, p. 1–16.

Ashley, G.M., Barboni, D., Domínguez-Rodrigo, M., Bunn, H.T., Mabulla, A.Z.P., Diez-Martín, F., Barba, R., and Baquedano, E., 2010a, Paleoenvironmental and paleoecological reconstruction of a freshwater oasis in savannah grassland at FLK North, Olduvai Gorge, Tanzania: Quaternary Research, v. 74, p. 333–343.

Ashley, G.M., Barboni, D., Domínguez-Rodrigo, M., Bunn, H.T., Mabulla, A.Z.P., Diez-Martín, F., Barba, R., and Baquedano, E., 2010b, A spring and wooded habitat at FLK Zinj and their relevance to origins of human behavior: Quaternary Research, v. 74, p. 304–314.

Ashley, G.M., Domínguez-Rodrigo, M., Bunn, H.T., Mabulla, A.Z.P., and Baquedano, E., 2010c, Sedimentary geology and human origins: a fresh look at Olduvai Gorge, Tanzania: Sedimentary Research, v. 80, p. 703–709.

Ashley, G.M., Deocampo, D.M., Kahmann-Robinson, J., and Driese, S.G., 2013, Groundwater-fed wetland sediments and paleosols: It's all about water table, *in* Driese, S.G., and Nordt, L.C., eds., New Frontiers in Paleopedology and Terrestrial Paleoclimatology: Paleosols and Soil Surface Analog Systems: SEPM, Special Publication 104, p. 47–61.

Ashley, G.M., Bunn, H.T., Delaney, J.S., Barboni, D., Domínguez-Rodrigo, M., Mabulla, A.Z.P., Gurtov, A.N., Baluyot, R.D., Beverly, E.J., and Baquedano, E., 2014, Paleoclimatic and paleoenvironmental framework of FLK North archaeological site, Olduvai Gorge, Tanzania: Quaternary International, v. 322–323, p. 54–65.

Baluyot, R.D., 2011, Paleoenvironmental reconstruction of a Pleistocene landscape, Olduvai Gorge, Tanzania [unpublished Undergraduate Honors thesis]: Rutgers University, 46 p.

Barboni, D., Ashley, G.M., Domínguez-Rodrigo, M., Bunn, H.T., Mabulla, A.Z.P., and Baquedano, E., 2010, Phytoliths infer locally dense and heterogeneous paleovegetation at FLK North and surrounding localities during upper Bed I time, Olduvai Gorge, Tanzania: Quaternary Research, v. 74, p. 344–354.

Bennett, C.E., Marshall, J.D., and Stanistreet, I.G., 2012, Carbonate horizons, paleosols, and lake flooding cycles: Beds I and II of Olduvai Gorge, Tanzania: Journal of Human Evolution, v. 63, p. 328–341.

Birney de Wet, C.C., and Hubert, J.F., 1989, The Scots Bay Formation, Nova Scotia, Canada, a Jurassic carbonate lake with silica-rich hydrothermal springs: Sedimentology, v. 36, p. 857–873.

Blumenschine, R.J., Peters, C.R., Masao, F.T., Clarke, R.J., Deino, A.L., Hay, R.L., Swisher, C.C., Stanistreet, I.G., Ashley, G.M., McHenry, L.J., Sikes, N.E., van der Merwe, N.J., Tactikos, J.C., Cushing, A.E., Deocampo, D.M., Njau, J.K., and Ebert, J.I., 2003, Lake Pliocene *Homo* and hominid land use from western Olduvai Gorge, Tanzania: Science, v. 299, p. 1217–1221.

Bowen, G.J., 2010, The Online Isotopes in Precipitation Calculator, http:/www.waterisotopes.org.

Brasier, M.D., 1980, Microfossils: London, George Allen and Unwin, 193 p.

Bunn, H.T., and Kroll, E.M., 1986, Systematic butchery by Plio-Pleistocene hominids at Olduvai Gorge, Tanzania: Current Anthropology, v. 27, p. 431–452.

Bunn, H.T., Mabulla, A.Z.P., Domínguez-Rodrigo, M., Ashley, G.M., Barba, R., Diez-Martín, F., Remer, K., Yravedra, J., and Baquedano, E., 2010, Was FLK North levels 1–2 a classic "living floor" of Oldowan hominins or a taphonomically complex palimpsest dominated by large carnivore feeding behavior?: Quaternary Research, v. 74, p. 355–362.

Bustillo, M.A., and Alonso-Zarza, A.M., 2007, Overlapping of pedogenesis and meteoric diagenesis in distal alluvial and shallow lacustrine deposits in the Madrid Miocene Basin, Spain: Sedimentary Geology, v. 198, p. 255–271.

Cabaleri, N.G., and Benavente, C.A., 2013, Sedimentary and paleoenvironments of the Las Caritas carbonate paleolake Canadon, Asfalto formation (Jurassic), Patagonia, Argentina: Sedimentary Geology, v. 284–285, p. 91–105.

Cerling, T.E., and Hay, R.L., 1986, An isotopic study of paleosol carbonates from Olduvai Gorge: Quaternary Research, v. 25, p. 63–78.

Cerling, T.E., and Quade, J., 1993, Stable carbon and oxygen isotopes in soil carbonates., *in* Swart, P.K., Lohmann, K.C., McKenzie, J., and Savin, S., eds., Climate Change in Continental Isotopic Records: American Geophysical Union, Geophysical Monograph 78, p. 217–231.

Colson, J., and Cojan, I., 1996, Groundwater dolocretes in a lake-marginal environment: an alternative model for dolocrete formation in continental settings (Danian of the Provence Basin, France) Sedimentology, v. 43, p. 175–188.

Coplen, T.B., Kendall, C., and Hopple, J., 1983, Comparison of stable isotope reference samples: Nature, v. 302, p. 236–238.

Dagg, M., Woodhead, T., and Rijks, D.A., 1970, Evaporation in East Africa: International Association of Scientific Hydrology, Bulletin, v. 15, p. 61–67.

Dawson, J.B., 2008, The Gregory Rift Valley and Neogene–Recent volcanoes of northern Tanzania: Geological Society of London, Memoirs, v. 33, 102 p.

de Wet, C.B., Mora, C.I., Gore, P.J.W., Gierlowski-Kordesch, E.H., and Cucolo, S.J., 2002, Deposition and geochemistry of lacustrine and spring carbonates in Mesozoic rift basins, Eastern North America, *in* Renaut, R.W., and Ashley, G.M., eds., Sedimentation in Continental Rifts: SEPM, Special Publication 73, p. 309–325.

Dean, W.E., and Fouch, T.D., 1982, Lacustrine Environment, *in* Scholle, P.A., Bebout, D.G., and Moore, C.H., eds., Carbonate Depositional Environments: American Association of Petroleum Geologists, Memoir 33, p. 98–130.

Deino, A.L., 2012, $^{40}Ar/^{39}Ar$ dating of Bed I. Olduvai Gorge, Tanzania, and the chronology of early Pleistocene climate change: Journal of Human Evolution, v. 63, p. 251–273.

Deino, A.L., Kingston, J.D., Glen, J.M., Edgar, R.K., and Hill, A., 2006, Precessional forcing of lacustrine sedimentation in the late Cenozoic Chemeron Basin, Central Kenya Rift, and calibration of the Gauss/Matuyama boundary: Earth and Planetary Science Letters, v. 247, p. 41–60.

Deocampo, D.M., 2002, Sedimentary processes and lithofacies in lake-margin groundwater-fed wetlands in East Africa, *in* Renaut, R.W., and Ashley, G.M., eds., Sedimentation in Continental Rifts: SEPM, Special Publication 73, p. 295–308.

Deocampo, D.M., 2004, Authigenic clays in East Africa: regional trends and paleolimnology at the Plio–Pleistocene boundary, Olduvai Gorge, Tanzania: Journal of Paleolimnology, v. 31, p. 1–9.

Deocampo, D.M., and Tactikos, J.C., 2010, Geochemical gradients and artifact mass densities on the lowermost Bed II eastern lake margin (~ 1.8 Ma), Olduvai Gorge, Tanzania: Quaternary Research, v. 74, p. 411–423.

Deocampo, D.M., Cuadros, J., Wing-Dudek, T., Olives, J., and Amouric, M., 2009, Saline lake diagenesis as revealed by coupled mineralogy and geochemistry of multiple ultrafine clay phases: Pliocene Olduvai Gorge, Tanzania: American Journal of Science, v. 309, p. 834–868.

Dickson, J.A.D., 1966, Carbonate identification and genesis as revealed by staining: Journal of Sedimentary Petrology, v. 36, p. 491–505.

Domínguez-Rodrigo, M., and Barba, R., 2007, A palimpsest at FLK North 1–2: independent carnivore- and hominid-made bone accumulations, *in* DomÍnguez-Rodrigo, M., Barba, R., and Egeland, C.P., eds., Deconstructing Olduvai: a Taphonomic Study of the Bed I Sites: Dordrecht, Springer, Vertebrate Paleobiology and Paleoanthropology, p. 127–164.

Domínguez-Rodrigo, M., Barba, R., and Egeland, C.P., 2007, Deconstructing Olduvai: a taphonomic study of the Bed I sites Vertebrate Paleobiology and Paleoanthropology Series: Dordrecht, Springer, 337 p.

Domínguez-Rodrigo, M., Mabulla, A.Z.P., Bunn, H.T., Diez-Martín, F., Barboni, D., Barba, R., Domínguez-Solera, S., Sánchez, P., Ashley, G.M., Baquedano, E., and Yravedra, J., 2010, Disentangling hominin and carnivore activities near a spring at FLK North (Olduvai Gorge, Tanzania): Quaternary Research, v. 74, p. 363–375.

Domínguez-Rodrigo, M., Pickering, T.R., Baquedano, E., Mabulla, A.Z.P., Mark, D.F., Musiba, C., Bunn, H.T., Uribelarrea, D., Smith, V., Diez-Martin, F., Pérez-González, A., Sánchez, P., Santonja, M., Barboni, D., Gidna, A., Ashley, G., Yravedra, J., Heaton, J., and Arriaza, M.C., 2013, First partial skeleton of a 1.34-milllion-year-old *Paranthropus boisei* from Bed II, Olduvai Gorge, Tanzania: PLOS One, v. 8.

Esteban, M., and Klappa, C.P., 1983, Subaerial exposure environment, *in* Scholle, P.A., Bebout, D.G., and Moore, C.H., eds., Carbonate Depositional Environments: American Association of Petroleum Geologists, Memoir 33, p. 2–95.

Ford, T.D., and Pedley, H.M., 1996, A review of tufa and travertine deposits of the world: Earth-Science Reviews, v. 41 p. 117–175.

Foster, A., Ebinger, C., Mbede, E., and Rex, D., 1997, Tectonic development of the northern Tanzanian sector of the East Africa Rift System: Geological Society of London, Journal, v. 154, p. 689–700.

Freytet, P., and Plaziat, J.C., 1982, Continental carbonate sedimentation and pedogenesis: Late Cretaceous and early Tertiary of Southern France: Contributions to Sedimentology, v. 12, p. 1–213.

Gasse, F., 1990, Tectonic and climatic controls on lake distribution and environments in Afar from Miocene to present, *in* Katz, B.J., ed., Lacustrine Basin Exploration, Case Studies and Modern Analogs: American Association of Petroleum Geologists, Memoir 50, p. 19–41.

Gasse, F., Fontes, J.C., Plaziat, J.C., Carbonel, P., Kaczmarska, I., De Deckker, P.D., Soulié-Marsche, I., Callot, Y., and Dupeuble, P.A., 1987, Biological remains, geochemistry and stable isotopes for the reconstruction of environmental and hydrological changes in the Holocene lakes from North Sahara: Palaeogeography, Palaeoclimatology, Palaeoecology, v. 60, p. 1–46.

Hay, R.L., 1976, Geology of the Olduvai Gorge: Berkeley, University of California Press, 203 p.

Hay, R.L., and Kyser, T.K., 2001, Chemical sedimentology and paleoenvironmental history of Lake Olduvai, a Pleistocene lake in northern Tanzania: Geological Society of America, Bulletin, v. 113, p. 1505–1521.

Hay, R.L., and Reeder, R.J., 1978, Calcretes of Olduvai Gorge and the Ndolanya beds of northern Tanzania: Sedimentology, v. 25, p. 649–673.

Hay, R.L., Pexton, R.E., Teague, T.T., and Kyser, T.K., 1986, Spring-related carbonate rocks, Mg clays, and associated minerals in Pliocene deposits of the Amargosa Desert, Nevada and California: Geological Society of America, Bulletin, v. 97, p. 1488–1503.

Hover, V.C., and Ashley, G.M., 2003, Geochemical signatures of paleodepositional and diagenetic environments: a STEM/AEM study of authigenic clay minerals from an arid rift basin, Olduvai Gorge, Tanzania: Clays and Clay Minerals, v. 51, p. 231–251.

Hurwitz, S., Stanislavsky, E., Lyakhovsky, V., and Gvirtzman, H., 2000, Transient groundwater–lake interactions in a continental rifts: Sea of Galilee, Israel: Geological Society of America, Bulletin, v. 112, p. 1694–1702.

Kampman, N., Burnside, N.M., Shipton, Z.K., Chapman, H.J., Nicholl, J.A., Ellam, R.M., and Bickle, M.J., 2012, Pulses of carbon dioxide emissions from intracrustal faults following climatic warming: Nature Geoscience, v. 5, p. 352–358.

Karis, A.M., Ashley, G.M., and Wright, J.D., 2012, Spatial and temporal variability of stable isotopes in an Upper Bed II tufa, Olduvai Gorge, Tanzania [abstract]: Geological Society of America, Abstracts with Program, v. 44, p. 239.

Katz, B.J., 1990, Lacustrine Basin Exploration, Case Studies and Modern Analogs: American Association of Petroleum Geologists, Memoir, v. 50, 340 p.

Kazancl, N.G., Gevrek, A.I., and Varol, B., 1995, Facies changes and high calorific peat formation in a Quaternary maar lake, central Anatolia, Turkey: the possible role of geothermal processes in a closed lacustrine basin: Sedimentary Geology, v. 94, p. 255–266.

Khalaf, F.I., 1990a, Occurrence of phreatic dolocrete within Tertiary clastic deposits of Kuwait, Arabian Gulf: Sedimentary Geology, v. 68, p. 223–239.

Le Gall, B., Nonnotte, P., Rolet, J., Benoit, M., Guillou, H., Mousseau-Nonnotte, M., Albaric, J., and Deverchere, J., 2008, Rift propogation at craton margin. Distribution of faulting and volcanism in the North Tanzanian Divergence (East Africa) during Neogene times: Tectonophysics, v. 448, p. 1–19.

Leakey, L.S.B., 1959, A new fossil skull from Olduvai: Nature, v. 184, p. 491–493.

Leakey, M.D., 1971, Olduvai Gorge: excavations in Beds I and II: 1960–1963: Cambridge, U.K., Cambridge University Press, v. 3, 306 p.

Liutkus, C.M., 2009, Using petrography and geochemistry to determine the origin and formation mechanism of calcitic plant molds: rhizolith or tufa?: Journal of Sedimentary Research, v. 79, p. 906–917.

Liutkus, C.M., and Ashley, G.M., 2003, Facies model of a semiarid freshwater wetland, Olduvai Gorge, Tanzania: Journal of Sedimentary Research, v. 73, p. 691–705.

Mack, G.H., Cole, D.R., and Trevino, L., 2000, The distribution and discrimination of shallow, authigenic carbonate in the Plio-Pleistocene Palomas Basin, Southern Rio Grande rift: Geological Society America, Bulletin, v. 112, p. 643–656.

Magill, C.R., Ashley, G.M., and Freeman, K.H., 2012a, Ecosystem variability and early human habitats in eastern Africa: Proceedings of the National Academy of Sciences, U.S.A.,v. 110, p. 1167–1174.

Magill, C.R., Ashley, G.M., and Freeman, K.H., 2012b, Water, plants, and early human habitats in eastern Africa: Proceedings of the National Academy of Sciences, U.S.A., v. 110, p. 1175–1180.

McCarthy, T.S., and Ellery, W.N., 1995, Sedimentation on the distal reaches of the Okavango fan, Botswana, and its bearing on calcrete and silcrete (ganister) formation: Journal of Sedimentary Research, v. 65, p. 77–90.

McHenry, L.J., 2005, Phenocryst composition as a tool for correlating fresh and altered tephra, Bed I, Olduvai Gorge, Tanzania: Stratigraphy, v. 2, p. 101–115.

McHenry, L.J., 2009, Element mobility during zeolitic and argillic alteration of volcanic ash in a closed-basin lacustrine environment: Case study Olduvai Gorge, Tanzania: Chemical Geology, v. 265, p. 540–552.

McHenry, L.J., Mollel, G.F., and Swisher, C.C., 2008, Compositional and textural correlations between Olduvai Gorge Bed I tephra and volcanic sources in the Ngorongoro Volcanic Highlands, Tanzania: Quaternary International, v. 178, p. 306–319.

Mees, F., 2002, The nature of calcareous deposits along pan margins in eastern central Namibia: Earth Surface Processes and Landforms, v. 27, p. 719–735.

Michel, L.A., Driese, S.G., Nordt, L.C., Breeker, D.O., Labotka, D.M., and Dworkin, S.I., 2013, Stable-isotope geochemistry of vertisols formed on marine limestone and implications for deep-time paleoenvironmental reconstructions: Journal of Sedimentary Research, v. 83, p. 300–308.

Mollel, G.F., Swisher, C.C., McHenry, L.J., Feigenson, M.D., and Carr, M.J., 2009, Petrogenesis of basalt–trachyte lavas from Olmoti Crater, Tanzania: Journal of African Earth Sciences, v. 54, p. 127–143.

Mollel, G.F., Swisher, C.C., III, Feigenson, M.D., and Carr, M.J., 2011, Petrology, geochemistry and age of Satiman, Lemagurut and Oldeani: sources of the volcanic deposits of the Laetoli Area, *in* Harrison, T., ed., Paleontology and Geology of Laetoli: Human Evolution in Context: Springer Science/Business Media, p. 99–119.

Monty, C.L.V., and Hardie, L.A., 1976, The geological significance of the freshwater blue-green algal calcareous marsh, *in* Walter, M.R., ed., Stromatolites: Amsterdam, Elsevier, Developments in Sedimentology, no. 20, p. 447–477.

Mount, J.F., and Cohen, A.S., 1984, Petrology and geochemistry of rhizoliths from Plio-Pleistocene fluvial and marginal lacustrine deposits, east Lake Turkana, Kenya: Journal of Sedimentary Research, v. 54, p. 263–275.

Olago, D., Opere, A., and Barongo, J., 2009, Holocene palaeohydrology, groundwater and climate change in the lake basins of the Central Kenya Rift: Hydrological Sciences Journal, v. 54, p. 765–780.

Olsen, P.E., 1986, A 40-million year lake record of early Mesozoic orbital climatic forcing: Science, v. 234, p. 842–848.

Peck, R.E., 1953, Fossil charophytes: The Botanical Review, v. 19, p. 209–227.

Pedley, H.M., 1990, Classification and environmental models of cool freshwater tufas: Sedimentary Geology, v. 68 p. 143–154.

Pedley, M., Andrews, J., Ordonez, S., Garcia del Cura, M.A., Gonzales Martin, J.-A., and Taylor, D., 1996, Does climate control the morphological fabric of freshwater carbonates? A comparative study of Holocene barrage tufas from Spain and Britain: Palaeogeography, Palaeoclimatology, Palaeoecology, v. 121, p. 239–257.

Pentecost, A., 2005, Travertine: Berlin, Springer-Verlag, 445 p.

Pla-Pueyo, S., Gierlowski-Kordesch, E.H., Viseras, C., and Soria, J.M., 2009, Major controls on sedimentation during the evolution of a continental basin: Pliocene–Pleistocene of the Guadix Basin (Betic Cordillera, southern Spain) Sedimentary Geology, v. 219, p. 97–114.

Platt, N.H., 1989, Lacustrine carbonates and pedogenesis: sedimentology and origin of palustrine deposits from the Early Cretaceous Rupelo Formation, W. Cameros Basin, N. Spain: Sedimentology, v. 36, p. 665–684.

Purvis, K., and Wright, V.P., 1991, Calcretes related to phreatophytic vegetation from the Middle Triassic Otter Sandstone of South West England: Sedimentology, v. 38, p. 539–551.

Quade, J., Chivas, A.R., and McCulloch, M.T., 1995, Strontium and carbon isotope tracers and the origins of soil carbonate in South Australia and Victoria: Palaeogeography, Palaeoclimatology, Palaeoecology, v. 113, p. 103–117.

Sikes, N.E., and Ashley, G.M., 2007, Stable isotopes of pedogenic carbonates as indicators of paleoecology in the Plio-Pleistocene (upper Bed I) western margin of Olduvai Basin, Tanzania: Journal of Human Evolution, v. 53, p. 574–594.

Spötl, C., and Wright, V.P., 1992, Groundwater dolocretes from the upper Triassic of the Paris Basin, France: a case study of an arid, continental diagenetic facies: Sedimentology, v. 39, p. 1119–1136.

Stewart, K.M., 1994, Early hominid utilisation of fish resources and implications for seasonality and behavior: Journal of Human Evolution, v. 27, p. 229–245.

Stewart, K.M., 1996, A report on the fish remains from Beds I and II sites, Olduvai Gorge, Tanzania: Kaupia Darmstadter Beitrage zur Naturgeschichte, v. 6, p. 263–269.

Stollhofen, H., Stanistreet, I.G., McHenry, L.J., Mollel, G.F., Blumenschine, R.J., and Masao, F.T., 2008, Fingerprinting facies of the Tuff IF marker, with implications for early hominin palaeoecology, Olduvai Gorge, Tanzania: Palaeogeography, Palaeoclimatology, Palaeoecology, v. 259, p. 382–409.

Suchecki, R.K., Hubert, J.F., and Birney De Wet, C.B., 1988, Isotopic imprint of climate and hydrogeochemistry on terrestrial strata of the Triassic–Jurassic Hartford and Fundy rift basins: Journal of Sedimentary Petrology, v. 58, p. 801–811.

Talbot, M.R., 1990, A review of the palaeohydrological interpretation of carbon and oxygen isotopic ratios in primary lacustrine carbonates: Chemical Geology, Isotope Geoscience Section, v. 80, p. 261–279.

Tandon, S.K., and Andrews, J.E., 2001, Lithofacies associations and stable isotopes of palustrine and calcrete carbonates: examples from an Indian Maastrichtian regolith: Sedimentology, v. 48, p. 339–355.

Tandon, S.K., and Friend, P.F., 1989, Near-surface shrinkage and carbonate replacement processes, Arran Cornstone Formation, Scotland: Sedimentology, v. 36, p. 1113–1126.

Tasch, P., 1973, Paleobiology of invertebrates: data retrieval from the fossil record: New York, John Wiley & Sons, 946 p.

Trauth, M.H., Maslin, M.A., Deino, A.L., Strecker, M.R., Bergner, A.G.N., and Duhnforth, M., 2007, High- and low-latitude forcing of Plio-Pleistocene East Africa climate and human evolution: Journal of Human Evolution, v. 53, p. 475–486.

Valero Garcés, B.L., Moreno, A., Navas, A., Mata, P., Machín, J., González Sampériz, P., Schwalb, A., Merellón, M., Cheng, H., and Edwards, R.L., 2008, The Taravilla Lake and tufa deposits (Central Iberian Range, Spain) as palaeohydrological and palaeoclimate indicators: Palaeogeography, Palaeoclimatology, Palaeoecology, v. 259, p. 136–156.

Received 27 November 2013; accepted 23 July 2014.